https://doi.org/10.5194/egusphere-2025-6178
Preprint. Discussion started: 18 December 2025

Petrogenesis and geodynamic implications of Ediacaran rocks from the Sirwa massif (Central Anti-Atlas); insights from U-Pb geochronology, whole-rock geochemistry, and Sm-Nd isotopes

Abdelhay Ben-Tami[1,2], Said Belkacim[1,6], Jamal El Kabouri[1], Bouchra Baidada[3], Joshua H.F.L. Davies[4], Morgann G. Perrot[5], Mohamed Bhilisse[2], Mohamed Assalmi[2], Mariam Ferraq[1,6], Mohamed Bouabdellah[7,8], David Lalonde[2].

[1] Laboratoire de Géologie Appliquée et Géo-Environnement, Département de la Géologie, Faculté des Sciences, Université Ibn Zohr, B.P.8106, Agadir, Maroc.
[2] Zgounder Millennium Silver Mining, Aya Gold and Silver Group, Rue De L'epargne, Quartier Racine, Casablanca, Maroc.
[3] Higher school of Technology, Fkih Ben Salah, Beni Mellal, Morocco.
[4] Department of Earth and Atmosphere Sciences, University of Quebec in Montreal, Montreal, QC H3C 3P8, Canada.
[5] Department of Earth and Planetary Sciences, McGill University, Montreal, Quebec H3A 0E8, Canada.
[6] Mining and Environmental Research Institute, University of Quebec in Abitibi-Timiskaming, Rouyn-Noranda, QC J9X 5E4, Canada.
[7] Laboratoire des Gîtes Minéraux, Hydrogéologie et Environnement, Faculté des Sciences, Université Mohammed Premier, 60000, Oujda, Maroc.
[8] Geology and Sustainable Mining Institute, Mohammed VI Polytechnic University, Benguerir 43150, Morocco.

Correspondence to: Abdelhay Ben-Tami (abdelhaybentami@gmail.com)

Abstract.

The geodynamic evolution of the Anti-Atlas belt post-Pan-African orogeny (~650 Ma) remains debated, particularly regarding the basement beneath the Central Anti-Atlas, and the geological processes leading to the formation of the Ediacaran Saghro Group (SG), and Ouarzazate Group (OG). New LA-ICP-MS U-Pb ages of 575 ± 3 Ma and 564 ± 2 Ma were obtained respectively from samples Zg-106, and Zg-119 from the OG. In addition, detrital zircons from SG sediments yield a prominent 2.1 Ga age peak, indicating local recycling of Paleoproterozoic basement material. Geochemically, two magmatic series are identified : (i) a SG mafic-intermediate calc-alkaline series with Nb-Ta and Ti negative anomalies from early back-arc basin setting; and (ii) a felsic-intermediate high-K calc-alkaline to shoshonitic series of the OG, exhibiting continental magmatic arc signatures. Isotope data (εNd (t): +3.2 to +4.5, TDM = 1431 - 1197 Ma for SG; εNd (t): -0.9 to +1.1, TDM = 1526– 1252 Ma for OG), indicates that the SG formed from a dominantly juvenile, mantle-derived source, with limited crustal contribution; while the slightly younger OG involved significant reworking of older, evolved continental crustal material.

These findings sustain a model where Early Ediacaran SG sediments and associated mafic-intermediate volcanics were formed in a back-arc basin. During this basin development, its shoulders were locally formed by the 2.1 Ga Paleoproterozoic basement, supplying Paleoproterozoic zircons to the Saghro host basin. This, further supports the occurrence of the Eburnian basement north of the Anti-Atlas Major Fault (AAMF). Additionally, the younger OG reflects a Late Ediacaran continental crust collapse event involving widespread crustal reworking and the emplacement of a Silicic Large Igneous Province (SLIP).

https://doi.org/10.5194/egusphere-2025-6178
Preprint. Discussion started: 18 December 2025

Keywords

Saghro Group; Ouarzazate Group; Sirwa massif; LA-ICP-MS U-Pb on zircon; 2.1 Ga Paleoproterozoic crust

1 Introduction

The Anti-Atlas belt of Morocco in the northern margin of the West African Craton (WAC) bears witness to a long-lived geological evolution started since the break-up of Rodinia. The Tonian - Cryogenian evolution of this belt record the establishment of a passive margin, and island arc which were accreted to the WAC margin at ca. 650 Ma, with the emplacement of syn-tectonic granitoids (Linnemann et al., 2019, 2014; Pereira et al., 2012a; Abati et al., 2010; Liégeois et al., 2006; Gasquet et al., 2005). The subsequent evolution of the Anti-Atlas belt during the Ediacaran is still debated despite the improvements in the understanding of the multiple events that prevailed during Neoproterozoic times (D'Lemos et al. 2006; Samson et al. 2004; Gasquet et al. 2008, 2005, 2004; Thomas et al. 2004, 2002; Ennih and Liégeois, 2008, 2001; Walsh et al. 2002), and led to the final amalgamation of Gondwana (D'Lemos et al., 2006; Gasquet et al., 2008, 2005). Within this time frame, and based on paleogeographic reconstruction and lithostratigraphic correlations; the Anti-Atlas belt was close to the Cadomian subduction system. In liaison, this subduction is responsible for the accretion of peri-Gondwana terranes and the final amalgamation of the Gondwana (El Kabouri et al., 2025; Rojo-Pérez et al., 2024; Stern, 2024; Garfunkel, 2015; Hefferan et al., 2014). However, it is still debated whether the Anti-Atlas records the post-collisional phase of the Pan-African belt, or if it is related to the establishment of a back-arc basin induced by the southward-dipping Cadomian subduction beneath the amalgamated WAC-Iriri/Tazigzaout arc complex at ca. 620 Ma (Errami et al., 2021a; Walsh et al., 2012; El Hadi et al., 2010; Abati et al., 2010). Furthermore, the nature of the basement north of the Anti-Atlas Pan-African suture zone, known as the Anti-Atlas Major Fault is also still a matter of debate. However, in the Zgounder Mine Region, a well-preserved section of Ediacaran sedimentation and magmatism provides key insights into the final stages of Pan-African tectono-magmatic evolution along the northern margin of the WAC.

The study area, so-called the "Zgounder Mine Region" in this contribution corresponds to the vicinity of the Zgounder Ag-Hg deposit (Ben-Tami et al., 2024). The Zgounder deposit is situated at approximately 265 km east of Agadir, and 220 km west of Ouarzazate, along the southern flank of the Ouzellagh-Sirwa Salient in the Central Anti-Atlas Mountains of the WAC. The Ediacaran period of the Zgounder Mine Region (630-539 Ma), is represented by : (i) the Saghro Group (SG) sedimentary successions and coeval mafic to intermediate units deposited at around 630 to 600 Ma (Abati et al., 2010); (ii) large felsic plutons, subvolcanic formations, along with coeval pyroclastic rocks referred to as the Ouarzazate Group (600 Ma - 539 Ma (Thomas et al., 2002).

We present new whole-rock geochemistry, and Sm-Nd isotopes for the Ediacaran successions of the Zgounder Mine Region. The aims are to decipher their petrogenesis, explore magma sources, and investigate their geodynamic significance in Ediacaran evolution of the WAC. We also report new LA-ICP-MS U-Pb dating on magmatic and detrital zircons to constrain

https://doi.org/10.5194/egusphere-2025-6178
Preprint. Discussion started: 18 December 2025

the lower Ediacaran magmatism and challenge the source of the Saghro Group's sedimentary units, hence, refining existing geodynamic models.

2 Geological setting

2.1 The Anti-Atlas belt

The Anti-Atlas Mountains, located on the northern edge of the WAC, and consist of a Proterozoic basement and a Late Ediacaran to Paleozoic cover (Leblanc and Lancelot, 1980) (Fig. 1B). These mountains record two major orogenic cycles: the Paleoproterozoic Eburnean and the Neoproterozoic Pan-African orogenies.

The Paleoproterozoic Eburnean orogeny is preserved in the Western Anti-Atlas, where low - to high-grade metamorphic rocks are intruded by a series of granitoids dated at ~2.2 Ga (Hefferan et al., 2014, and references therein; O'Connor et al., 2010; El Hadi et al., 2010; Ennih and Liégeois, 2008; Gasquet et al., 2008, 2005; Thomas et al., 2002; Walsh et al., 2002; Aït Malek et al., 1998). Overlying these terranes, is the carbonate and quartzite succession of the Taghdout Group deposited in a passive margin (Errami et al., 2021a; Álvaro et al., 2014; Abati et al., 2010; Thomas et al., 2004). U-Pb ages on a quartzite sample from the Taghdout Group provided ages spanning from 2182 to 1987 Ma (Walsh et al., 2012). Moreover, undeformed Doleritic dikes intrude the Taghdout Group in the Ighrem and Zenaga inliers, and were dated between 1710 and 1630 Ma by Ikenne et al., (2017), and Ait Lahna et al., (2020), respectively. Overall, this implies that the Taghdout Group is in fact of Paleoproterozoic in age (Ikenne et al., 2017; Abati et al., 2010).

The Neoproterozoic episode known as the Pan-African orogeny is well established in the Central and Eastern Anti-Atlas (ca. 760 to 550 Ma) in numerous studies (Bouougri et al., 2020; Soulaimani et al., 2018; Triantafyllou et al., 2016; Karaoui et al., 2015; Blein et al., 2014; Álvaro et al., 2014; Hefferan et al., 2014; Walsh et al., 2012; El Hadi et al., 2010; Errami et al., 2009; Michard et al., 2008; Gasquet et al., 2008, 2005; Ennih and Liégeois 2008, 2001; Thomas et al., 2004, 2002). These Pan-African successions start with an early Tonian - Cryogenian syn-rift units, consisting of carbonates and quartzites known as the Jbel Lkst Group (Kerdous inlier), the Tachdamt Group (Zenaga inlier), and the Bleida quartzites (Bou-Azzer-El Graara inlier) (Álvaro et al., 2014). The rifting process is evidenced by the formation of oceanic basement now preserved as ophiolitic sequences in the Bou-Azzer and Sirwa inliers (Thomas et al., 2002, 2004). Concurrently, a long-lived island arc complex formed north of the WAC (Admou et al., 2012; D'Lemos et al., 2006; Thomas et al., 2002, 2004). This arc is now preserved as the 743 ± 14 Ma Iriri Arc in the Sirwa inlier (Thomas et al., 2002), and its equivalent, the Tazigzaout-Bougmane Complex in the Bou-Azzer inlier, dated at 752 ± ^{1}-$_{2}$ Ma (D'Lemos et al., 2006). Following this, and as the north dipping subduction ceased, these latter terranes were subsequently deformed and obducted to the northern margin of the WAC around 650 Ma during the main Pan-African orogeny (Hefferan et al., 2014, and references therein; Thomas et al., 2002). Further, widespread calc-alkaline magmatic intrusions and regional metamorphism affected the Anti-Atlas belt (Hefferan et al., 2014, and references therein), with several syn-orogenic granitoids dated between 680 and 640 Ma (Hefferan et al., 2012; Walsh et al., 2012; El Hadi et al., 2010; Inglis et al., 2005; Thomas et al., 2002).

https://doi.org/10.5194/egusphere-2025-6178
Preprint. Discussion started: 18 December 2025

In the northeastern domain of the Anti-Atlas, the Ediacaran stratigraphy (630 – 539 Ma) comprises an early Ediacaran basement of Saghro Group, consisting of folded meta-sedimentary units under greenschist facies conditions, and covered by a late-Ediacaran Ouarzazate Group sequence of volcanic and volcano-sedimentary nature (Ouabid and Garrido, 2023; Errami et al., 2021a; Yajioui et al., 2020; Michard et al., 2017; Blein et al., 2014; Álvaro et al., 2014, 2014b; Walsh et al., 2012; Abati et al., 2010; Errami et al., 2009; Gasquet et al., 2008; Liégeois et al., 2006; Thomas et al., 2002; Fekkak et al., 2001; Bajja, 2001; Ouguir et al., 1996). The transition from volcanic dominated successions of the Ouarzazate Group to the establishment of a stable platform series is recorded during the Ediacaran - Cambrian transition, with the deposition of the Taroudante and Tata groups in an anorogenic setting (Álvaro et al., 2014).

https://doi.org/10.5194/egusphere-2025-6178
Preprint. Discussion started: 18 December 2025

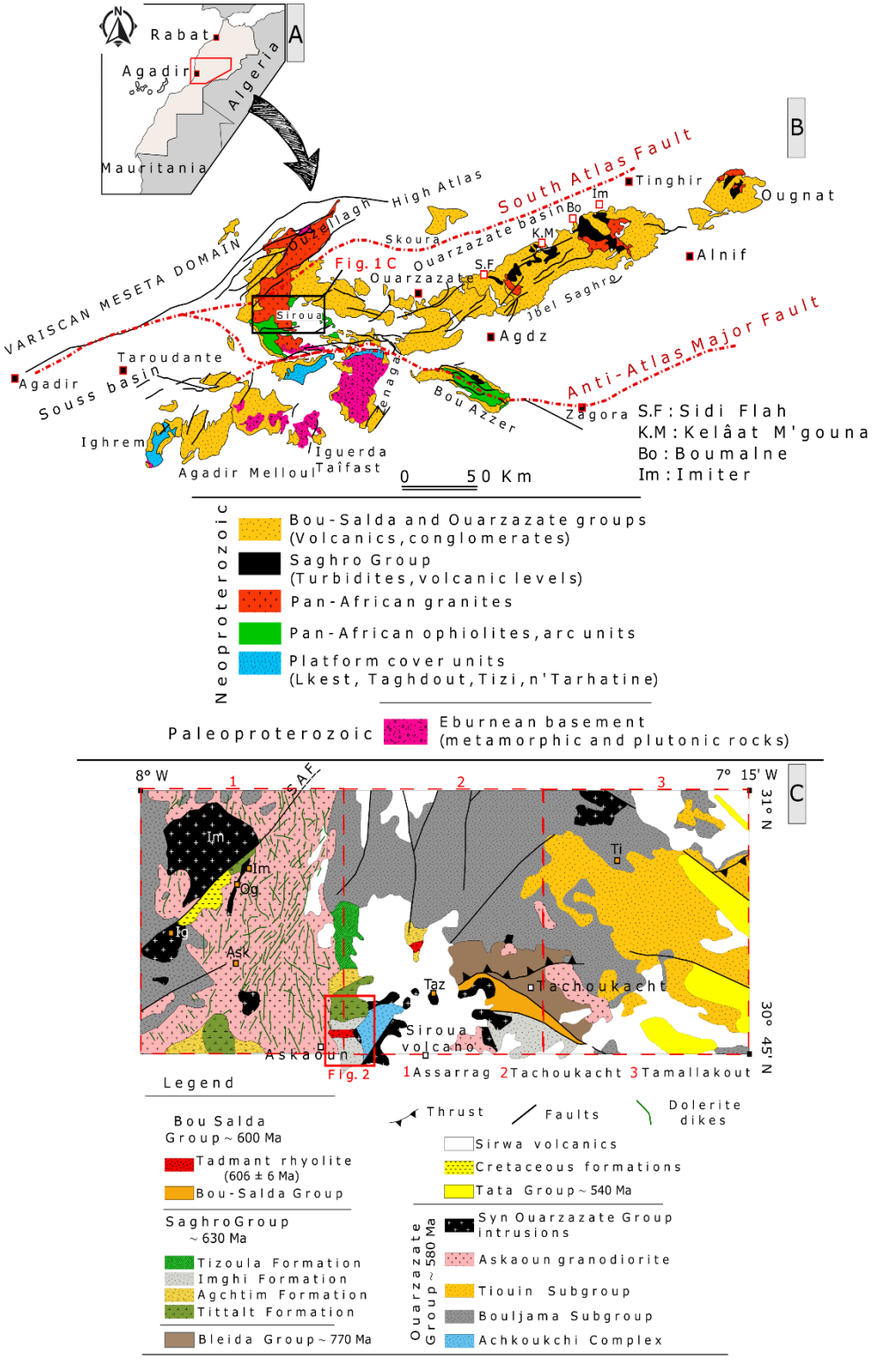

https://doi.org/10.5194/egusphere-2025-6178
Preprint. Discussion started: 18 December 2025

Figure 1: (A) Sketch map locating the Anti-Atlas belt in respect to Morocco (Saadi, 1985). (B): geological map of the Central and Eastern Anti-Atlas Proterozoic inliers (redrawn and modified after Michard et al., (2017)). (C): Schematic representation of the geology of the Sirwa massif (compiled and redrawn after Thomas et al., (2002)); location of the Zgounder Mine Region in red square (see Fig. 2). Abbreviations: Taz : Tazoult quartz-porphyry (559 ± 6 Ma); Im: Imourkhssen granite (562 ± 5 Ma); Ti: Tikhfist rhyolite (571 ± 8 Ma); Ask: Askaoun granodiorite (575 ± 8 Ma); Ig: Ighrem granite; Og: Ougougane granite; and SAF: South Atlas Fault. U-Pb ages are from Thomas et al., (2002).

2.2 Sirwa inlier

The recent geological mapping of 1/50 000 scale sheet maps of Douar Çour, Assarrag, Tachoukacht, Tamallakout, Sirwa, Taghdout, and Açdif (see Fig. 1C for relevant sheets) has subdivided the Sirwa inlier into various groups (Thomas et al., 2000a; De Beer et al., 2000; Gresse et al., 2000).

Paleoproterozoic rocks are the oldest in the Sirwa inlier, mainly composed of altered iron-rich gneiss and schist fragments from the Zenaga Complex (Thomas et al., 2002). The Tachdamt Group's sedimentary and volcanic rocks were deposited after Rodinia's breakup (Thomas et al., 2002). Interbedded Tachdamt Group volcaniclastic deposits date to ca. 883 Ma (Bouougri et al., 2020). This Group is overlain by the Khzama Complex, which includes the Tasriwine ophiolite, the Iriri Migmatite, and Tachoukacht schists formed during island arc development and associated back-arc oceanic crust (Thomas et al., 2002).

The Saghro Group, as defined by Thomas et al., (2002), is a thick, ~8000 m pile of deformed sedimentary, volcanoclastic, and volcanic rocks with a calc-alkaline composition and greenschist-facies metamorphism. It includes six lithostratigraphic formations: Tittalt, Agchtim, Tizoula, Imghi, Azarwas, and Tafiat. The lower sequence features greywacke/turbidites with volcanic rocks, while the upper formations consist of coarse-grained clastic rocks (Thomas et al., 2002). The age of the Saghro Group has been constrained by Liégeois et al., (2006) and Abati et al., (2010) using U-Pb dating on detrital zircons from both the Sirwa and Saghro massifs. These studies established a maximum depositional age at approximately 610 Ma. More recent data from the Eastern Saghro massif reported by Errami et al., (2021a), provided slightly younger detrital ages clustering around 607 ± 6 Ma and 604 ± 5 Ma. In addition, the entire Saghro series was intruded by syn-tectonic granitoids dated at 603 ± 6 Ma and 600 ± 3 Ma (Errami et al., 2021a). Crucially, in the Sirwa inlier, the Saghro Group is significantly older as it is intruded by the Mzil granite dated at 614 Ma (Thomas et al., 2002, 2004).

The Bou Salda Group is a thick volcano-sedimentary succession from 610 to 580 Ma (Belkacim et al, 2017; Gasquet et al., 2008), interpreted as basin infills of grabens and pull-apart basins within the AAMF (Errami et al., 2021a; Gasquet et al., 2008; Thomas et al., 2002). In the Sirwa inlier, it mainly comprises the Lmakhzene and Ighil members (Thomas et al., 2002). The Lmakhzene Member features arkosic gritstones, sandstones, and conglomerates, while the volcanic Ighil Member includes basalt, rhyolite, and andesite. Ages for the Bou Salda Group in the Sirwa inlier are derived from the Tadmant and Tamriwine rhyolites, dated respectively at 606 ± 6 Ma and 605 ± 9 Ma (Thomas et al., 2002) (Fig. 1C, and Fig. 2). Pelleter et al. (2016), also dated the Tadmant rhyolite at 610 ± 7 Ma (Fig. 2). Nonetheless, Abati et al., (2010) reported detrital zircon ages of 600 ± 12, 603 ± 13, and 625 ± 12 Ma, suggesting a maximum age for quartzite clasts in a conglomerate and, hence for the Bou Salda Group.

https://doi.org/10.5194/egusphere-2025-6178
Preprint. Discussion started: 18 December 2025

The Ouarzazate Group sequences (580-539 Ma; Blein et al., 2014b; Toummite et al., 2013; Thomas et al., 2004) of immature, coarse clastic sedimentary rocks (conglomerates, arkoses, reworked volcanic rocks) acid to intermediate volcaniclastic rocks (lapilli tuff, volcanic breccias, ignimbrites, etc.) and lavas (minor basalt, andesite and rhyolite) are associated with post-collisional high-K calc-alkaline to shoshonitic magmatism (Soulaimani et al., 2018). Briefly, throughout the Sirwa inlier, the
145 Ouarzazate Group is subdivided into four subgroups (Fig. 1C for relevant groups) (Tiouin, Bouljama, Tafrant and Achkoukchi) (Thomas et al., 2000a; Gresse et al., 2000; De Beer et al., 2000). Under an extensional regime, typical foreland basin successions of Tata Group were deposited, following the post-orogenic molasse volcaniclastic rocks of the Ouarzazate Group (Thomas et al., 2002) (Fig. 1C).

https://doi.org/10.5194/egusphere-2025-6178
Preprint. Discussion started: 18 December 2025

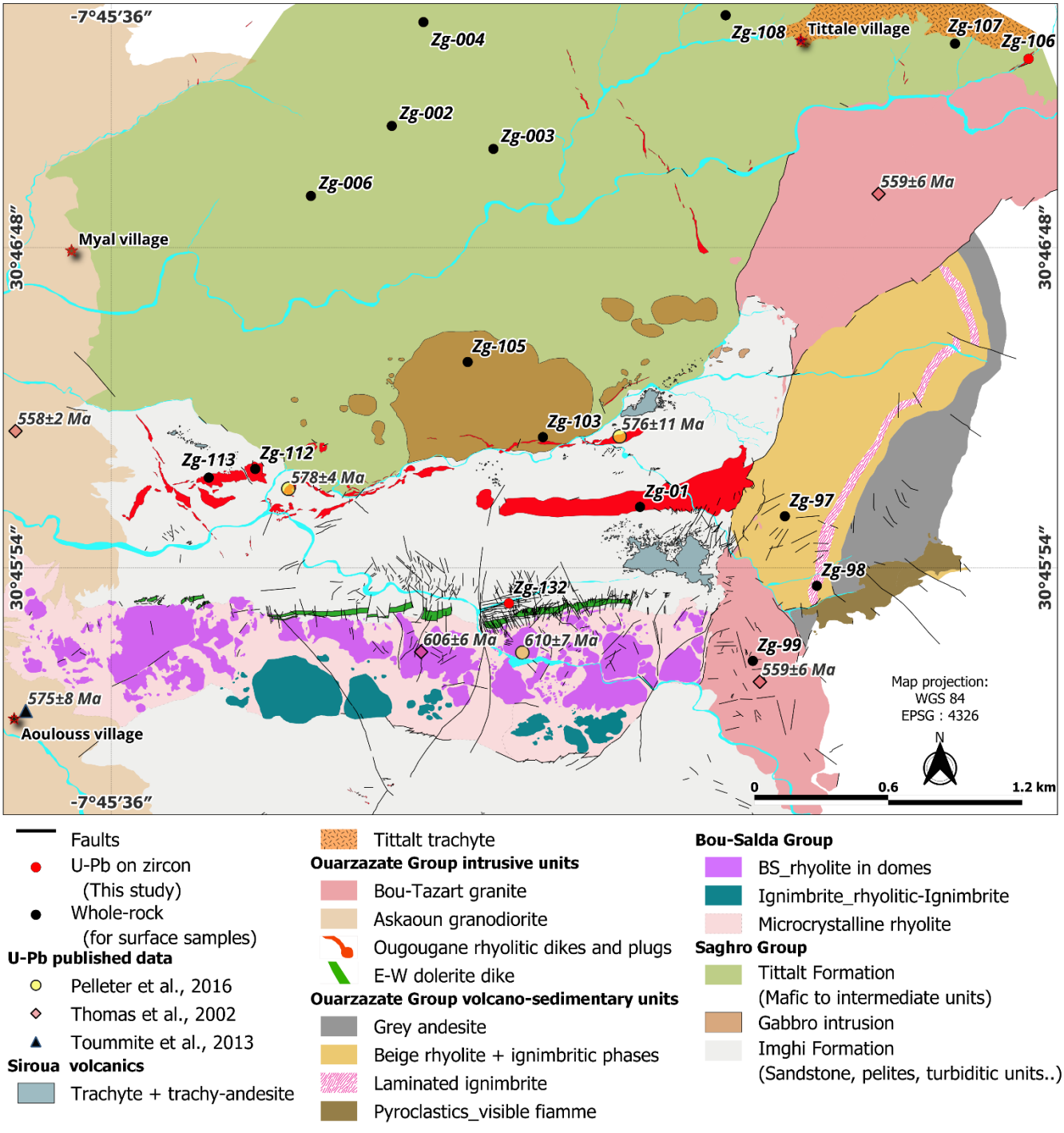

Figure 2: Detailed geological map of the Zgounder Mine Region (this study). Locations of surface samples are indicated on the map. Underground samples (e.g. Mine levels, drill holes) including the dated Zg-119 are not represented on the map.

https://doi.org/10.5194/egusphere-2025-6178
Preprint. Discussion started: 18 December 2025

3 Data and methodology

3.1 U-Pb zircon geochronology

Three samples from the Zgounder Mine Region (Zg-106; Zg-119; Zg-132) were selected for U-Pb zircon geochronology (see Fig. 2 for location: Zg-106, and Zg-132). They were crushed, sieved to 50-250 µm, and weighed (1.4 kg for Zg-106; 1.5 kg for Zg-119; 2.3 kg for Zg-132), at the preparation unit of the Département de Géologie, Faculté des Sciences, Université Ibn Zohr, Maroc. Samples were then shipped to the Geotop Research Center, Université de Québec à Montréal (UQAM), Canada. Analytical parameters are detailed in supplementary data 1, following Horstwood et al. (2016) (refer to table 1 in supplementary data 1). Ages of intrusive rocks are reported as weighted mean $^{206}Pb/^{238}U$ dates, and detrital zircon data as concordia dates. LA-ICP-MS U-Pb data are in supplementary table 5.

3.2 Whole-rock geochemistry and Sm-Nd isotopes

Fresh rock samples were collected for whole-rock geochemistry and Sm-Nd isotopes from outcrops (surface and underground), as well in various diamond drill holes from the Zgounder Mine Region. Crushing and powdering of the rock samples were performed at the facilities of the Zgounder Millennium Silver Mining Company (ZMSM). For each sample, lithostratigraphic position, sample type, drill core name and depth, short description and analytical methods applied are reported in supplementary table 3. Further details on the analytical procedures are given as supplementary data 2.

4 Results

4.1 Petrography

4.1.1 The Saghro Group rocks

- The Saghro Group is mainly represented by fine to medium-grained, and dark to olive green mafic volcanic rocks. They contain fine-grained plagioclase and clinopyroxene phenocrysts dispersed in the groundmass (Fig. 3). A medium- to coarse-grained equigranular and dark green gabbroic facies is also present, and shows heavily altered pyroxenes and amphiboles (Fig. 3a). Dolerite sample (Fig. 3b) have an intergranular texture, with lath shaped plagioclase, primary Fe-Ti oxides, and clinopyroxene aggregates. Sample Zg-108 is andesitic in composition (Fig. 3c), and shows a medium-grained intergranular texture. The texture is microlitic to microlitic-porphyritic for basalt and basaltic-andesite samples (Fig. 3d).
- The dated sandstone sample (Zg-132), displays distinct well-defined, millimeter-scale laminations, controlled by compositional variations. Darker bands are enriched in chlorite, whereas lighter laminae are mainly composed of quartz and muscovite (Fig. 3e). Such alternating patterns suggest fluctuating depositional conditions, specifically changes in hydrodynamic energy and the amount of clay input, consistent with a low-energy, suspension-dominated sedimentation typical of distal turbidites or quiet shallow-marine environment.

https://doi.org/10.5194/egusphere-2025-6178
Preprint. Discussion started: 18 December 2025

4.1.2 The Ouarzazate Group rocks

- Rhyolite samples show a microcrystalline locally glassy texture. Primary mineral assemblages are composed of quartz megacrysts and, K-feldspar altered to albite, and embedded in a devitrified matrix. Secondary alteration minerals are sericite, albite, with some local carbonate veinlets (Fig. 3f). Dolerite samples (Zg-13, Zg-15; Fig. 3g) are fine-grained, exhibiting an intergranular texture. Plagioclase crystals, locally transformed to albite are moderately sericitized and rarely altered to epidote, with equant opaque grains enclosed in the primary minerals (plagioclase, pyroxene). A dolerite sample (Zg-14) collected next to the mineralized zone have an intergranular texture in which laths of black oxidized plagioclase were included in pyroxene crystals (Fig. 3h). The plagioclase crystals are strongly altered and replaced by a mixture of blue chlorite, weak and sparse grains of epidote. Clinopyroxene is mainly replaced by hornblende and actinolite, and partially by pyrite. Ignimbrite samples show an eutaxitic texture with remarkable fiamme and dense welded volcanic glass, along with cryptocrystalline facies locally fluidal, mainly composed of quartz, opaque minerals, sericitized phenocrysts of plagioclase and K-feldspars (Fig. 3i).
- Granodiorite and quartz-diorite samples are grey to light brown with a moderate pinkish tint related to K-feldspar alteration, and they show a homogenous coarse-grained texture. Sericite and clay minerals replace lath-shaped plagioclase phenocrysts, and are associated with chlorite and iron oxides (Fig. 3g). Chlorite replaces biotite, which locally substitutes hornblende crystals. Opaque minerals are enclosed in hornblende, biotite and plagioclase. Granite is medium- to locally fine-grained; it is distinguished from the granodiorite and quartz-diorite by its white to pink color (Fig. 3k).

https://doi.org/10.5194/egusphere-2025-6178
Preprint. Discussion started: 18 December 2025

Lithology	Sample code	Texture	Primary minerals and accessory phases (size + %)	Alteration minerals
Saghro Group rocks				
Gabbro	Zg-103 Zg-105	medium to coarse-grained/ locally equigranular	Olivine (<0,1mm; <2%); Pyroxene (up to 0,25mm; less than 5%); hornblende;(5-13%); Ca-rich plagioclase (20-35%); Fe-Ti oxides (up to 9%); accessory sulfides (pyrite); <2%)	Secondary Amphibole; Green Chlorite as patches (10%); Sericite (up to 15%); epidote (2%)
Dolerite	Zg-107	intergranular	Clinopyroxene, up to 0,5mm; up to 15%); Plagioclase (20-35%); primary Fe-Ti oxides (up to 12%).	Chlorite; minor epidote; rare albite; minor sericite (green schist alteration package)/ secondary amphibole,
Andesite	Zg-108	Medium-grained intergranular	Primary Fe-Ti oxides (up to 10%); Pyroxene (up to 0,2mm; less than 5%); Plagioclase (up to 35%)	Minor sericite, oxides.
Basaltic-andesite	Zg-002	Microlitic-porphyritic	Clinopyroxenes as fine aggregates (0,1mm; up to 10%); Automorphic plagioclase as micro and phenocrysts locally zoned (0,4 - up 1,4 mm; up to 40%); Opaque minerals (<5%)	Chlorite (micro-patches); Sericite (13%); Argillic alteration, minor kaolinite in plagioclase, oxides altering plagioclase.
	Zg-003 Zg-004		Micro and local phenocrysts of Pyroxene (0,1 – to up to 1 mm; up to 13%); Plagioclase as micro and phenocrysts locally zoned (0,4 - up to 1,4 mm; 35%); oxides altering plagioclase phenocrysts; rare apatite	Chlorite; dispersed calcite (up to 5%), oxide orioles surrounding pyroxenes; Sericite (14%);
Basalt	Zg-006	Microlitic-porphyritic	Pyroxene (0,1 - 0,8 mm; less than 10%); Micro plagioclase in the mesostasis + phenocrysts (0,2-1,5mm; 30-38%); Fe-Ti oxides.	Abundant calcite, secondary quartz (amygdales); Sericite.
Sandstone	Zg-132	Fine to medium-grained	Compositional variation for darker/lighter laminations: Quartz (0,2-0,4mm; up to 70%); muscovite flakes (10 to 30 %); chlorite (10 to 25 % or more); feldspar (up to 0,3mm); iron oxides (7%).	
Ouarzazate Group rocks				
Rhyolite	Zg-04 Zg-06 Zg-117	Cryptocrystalline, locally glassy with visible fiamme	Quartz (0, 2-0,4mm; up to 30%); Plagioclase (0, 15-0,6mm; 20-30%); K-feldspar (0, 15-0,8mm; up to 55%); Biotite (~0,1mm; less than 4%); Primary opaque minerals; Zircon (<1%) + xenoliths (1-2mm; 6%)	Slight albitization; Chlorite/muscovite (micro-patches); Sericite;
Rhyolitic-ignimbrite	Zg-05 Zg-111	vitroclastic to cryptocrystalline texture, locally fluidal	Quartz (0,1-1,8 mm; up to 30%); Plagioclase (up to 2,2mm); K-feldspar (0,8-1,9mm); Fe-Ti oxides (less than 4%); + xenoliths (meta-sedimentary facies)	Sericite (4-8%)
Porphyritic rhyolite	Zg-110	porphyritic	Quartz in phenocrysts (1-4,5mm; 18-28%); K-feldspar (up to 4,5 mm); Plagioclase (up to 4,3 mm); Opaque minerals (Less than 5%); + visible xenoliths (up to 2,6mm)	Sericite (3-6%); Muscovite (1-2%)
Quartz-diorite	Zg-07	medium to coarse-grained	Amphibole (0, 15-1mm; 2-8%) ; Biotite (0,25-2mm ; 4-9%) ; Plagioclase (1,3 – 3.4 mm; 32-60%); K-feldspar (up to 1,6m ; up to 8%) ;	Chlorite (5-8%); Muscovite (3%); Epidote (<2%)

https://doi.org/10.5194/egusphere-2025-6178
Preprint. Discussion started: 18 December 2025

			interstitial quartz (0.2 -1.2 mm; up to 25 %); Primary opaque minerals (inclusion in amphibole crystals; <6%); Zircon (<1%)	Sericite (10-15%); Kaolinite and Clay minerals (2%); Oxides (6%);
Granodiorite	Zg-08 Zg-09	medium to coarse-grained, isogranular texture	Hornblende (0,15-1,2mm ; 6-10%) ; minor Biotite (0,25-2mm ; 4-18%) ; Plagioclase phenocrysts (0.25 – 2.6 mm; 45-55%); Orthoclase (1-2,2m ; 20-35%) ; Quartz (0.4 -2.5 mm; 10-30 %); +xenoliths ; Primary + secondary opaque minerals ; Zircon in biotite (<1%)	Chlorite (less than 10%); Sericite (up to 25%); Epidote (2%);; Clay minerals (2%); Kaolinite (<2%); Oxides (4%)
Dolerite	Zg-13 Zg-15	intergranular	Clinopyroxene (augite) (0,1mm; up to 6%); brown hornblende (up to 14%); automorphic plagioclase (0,4 - less than 1,4 mm; up to 43%); Biotite (<4%); secondary Quartz (0,1-0,4mm; <4%); Primary opaque minerals (<5%); accessory sulfides (pyrite); <2%)	Intense Chlorite (patches); Sericite (20%); Muscovite (up to 2%)
Diabase	Zg-14	intergranular	Pyroxene (0,03-0,1mm; less than 10%); Plagioclase (0,25-2,5mm; 35-40%); Fe-Ti oxides (magnetite+ilmenite prisms, <6%)	Patches of blue chlorite (0,25-1,1 mm; up to 38%); sericite (up to 8%); clay minerals (<6%); Secondary amphibole
Ignimbrite	Zg-97 Zg-98	eutaxitic texture with visible fiamme	Quartz (less than 0,7mm; 45-60%); Plagioclase; K-feldspar (sanidine; up to 23%, 0,4mm); Opaque minerals (euhedral to subhedral) (5-10%); + Xenoliths (anhedral); Zircon in inclusion in k-feldspar crystals (<1%)	Sericite (less than 5%); Scarce chlorite (2%); Kaolinite (5%)
Granophyre	Zg-99	coarse grained	Amphibole; sub-automorphic Biotite (0,4-0,9mm) ; Plagioclase (up to 8%; 0,5–1mm) ; K-feldspar (microcline) ; Quartz (rounded and eye-shaped (0,4-3,2mm)); Magnetite + apatite+ Zircon (<2%) (; +xenoliths (mafic)	Chlorite; Sericite ; Muscovite
Rhyolite	Zg-106	Microcrystalline, locally fluidal	Quartz (0,2-0,4mm) ; K-feldspar (up to 0,3mm); Plagioclase (< 0,4mm); + rare xenoliths (mafic to intermediate). Mesostasis forms more than 85% of the rock.	Albite; Chlorite (3-5%); Sericite (up to 25%); Calcite (veinlets) (2%)
Granite	Zg-115 Zg-119	medium to fine-grained, equigranular	Amphibole (rare 2% (<0,2mm); Biotite (up to 2%); Microcline with visible twinning (20-30% (0,5 to 1,2 mm)); Plagioclase (6-10% (=0,7mm)); Quartz (35-45% (0,4 to 1,3 mm)) ; +metasedimentary xenoliths (0,5-1cm; 3%) ; Opaque minerals; Zircon (<2%);	Chlorite (moderate); Actinolite (less amount); Sericite (15%); Muscovite (less than 4%)
Rhyolite	Zg-01 Zg-112 Zg-113	microcrystalline porphyritic texture,	Quartz phenocrysts (0,4-0,9mm); Plagioclase; K-feldspar; rare biotite Opaque minerals + rare xenoliths	Muscovite rare micro-patches; Sericite (up to 12%)
Micro-granite	Zg-02 Zg-03	fine to medium-grained texture	Amphibole (0,1-0,4mm; rare: less than 3%); Biotite (<0,9mm; 2-4%); Quartz (0,4-3,2mm; less than 40%); K-feldspar (up to 32%); Plagioclase (1-2,9mm; up to 20%); Opaque minerals (<4%); + xenoliths (up to 4,5mm)	Abundant Sericite (up to 10%); chlorite (<3%); rare epidote (<1%)
	Zg-109	fine grained texture	Amphibole (0,1-0,4mm; rare: less than 3%); Biotite (<0,5mm; 2-4%); Quartz (0,4-0,9mm; less	Abundant Sericite (up to 10%); chlorite (<3%); rare epidote (<1%)

https://doi.org/10.5194/egusphere-2025-6178
Preprint. Discussion started: 18 December 2025

			than 48%); K-feldspar (up to 30%); Plagioclase (0,5-1,4mm; up to 22%); Opaque minerals (<4%)	

Table 1: Mineralogical compositions of the studied rocks of the Saghro Group and Ouarzazate Group from the Sirwa massif (Zgounder Mine Region; 33 samples), refer to Fig. 2 for surface sample's locations.

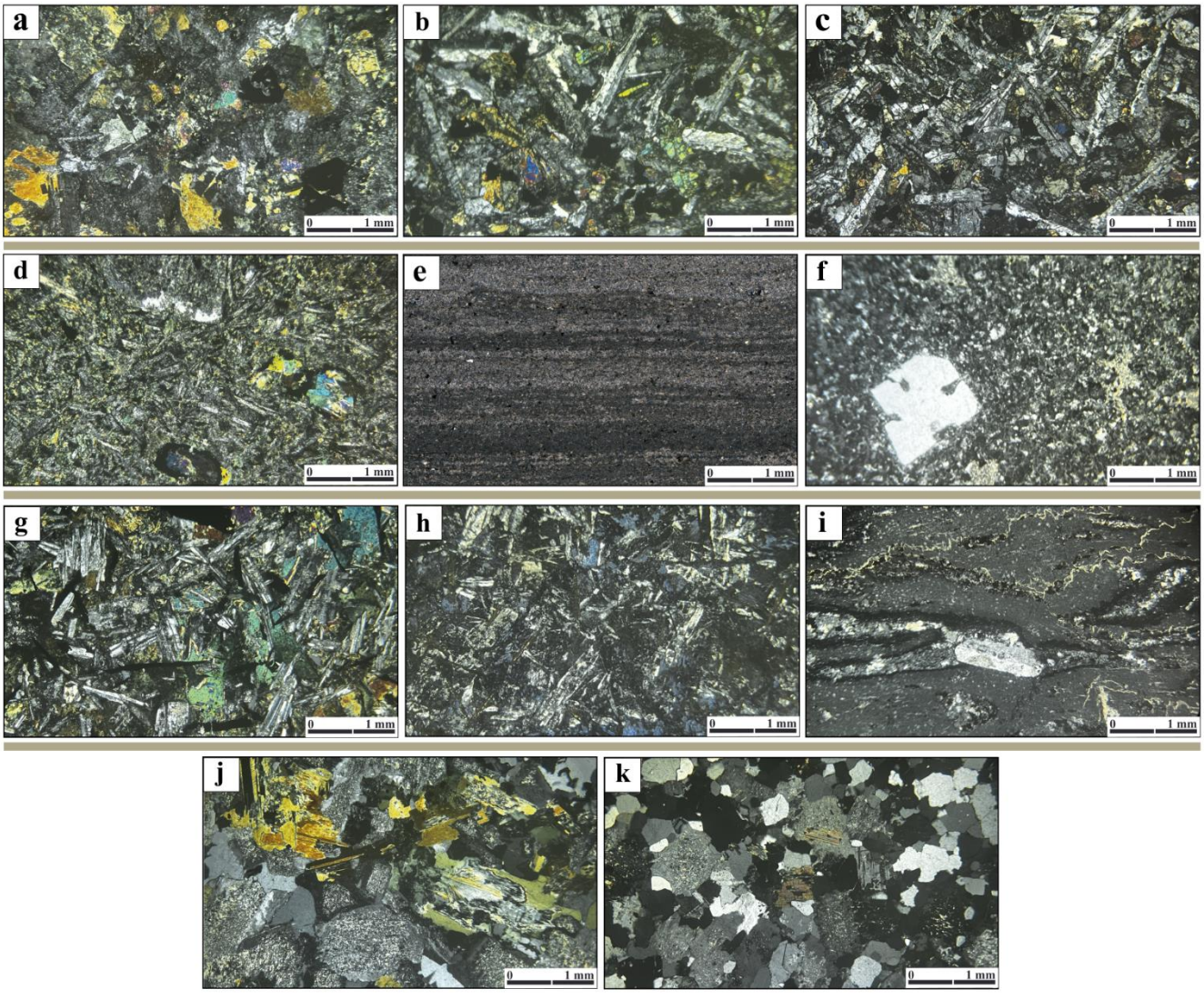

Figure 3: Photomicrographs (all in cross-polarized light) of the studied Saghro Group and Ouarzazate Group rocks. (a) Gabbro sample showcasing a medium to coarse- grained locally equigranular texture. (b) An intergranular texture for dolerite. (c) Andesite with a medium grained intergranular texture. (d) Microlitic-porphyritic texture for basaltic-andesite. (e) Sandstone (Zg-132) exhibiting millimetre-scale laminations showcasing darker bands enriched in chlorite, with quartz-muscovite lighter laminations. (f) Microcrystalline texture for rhyolite with embayed quartz phenocrysts. (g) Dolerite exhibiting an intergranular texture . (h) Diabase characterized by an intergranular texture with patches of blue chlorite. (i) Welded ignimbrite with an eutaxitic texture displaying flow textures with feldspars (sanidine) crystals embedded in a glassy fiamme. (j) Quartz diorite with subhedral to anhedral amphiboles and sericitized plagioclase. (k) Medium to locally fine-grained granite, with an anhedral to subhedral equigranular texture.

https://doi.org/10.5194/egusphere-2025-6178
Preprint. Discussion started: 18 December 2025

4.2 Cathodoluminescence (CL) imaging and LA-ICP-MS U-Pb zircon geochronology

4.2.1 Tittalt rhyolite (Zg-106)

The rhyolite sample Zg-106 was taken from the Tittalt Formation as the lower unit that represents the Saghro Group in the Sirwa massif (Thomas et al., 2002, 2004). For context, this rhyolite is represented as a compact and homogenous body of approximately 46 m length, and 4 to 5 m thick. On the field, it corresponds to a rhyolitic dike crosscutting the mafic to intermediate units of the Tittalt Formation (Fig. 2). Admittedly, similar subvolcanic activity represented by E-W-trending rhyolitic dikes and related plugs was previously reported in the Zgounder Mine Region by Pelleter et al., (2016), and attributed to the Assarrag suite of Thomas et al., (2002). On the outcrop, it has a light pink to brownish taint with visible laminations. U-Th ratios range between 0.3 and 1. Most of the zircon crystals in this sample are euhedral and moderate in size. CL images reveal that zircon grains exhibit typical oscillatory zoning with rare and limited dark rim overgrowths (Fig. 4-1a), with no indication of inherited zircon grains. For filtering the data, only zircons with 95% to 105% concordance were used for age calculation (Fig. 4-1b). Thus, the weighted mean age for this sample gave 575 ± 3 Ma (MSWD = 1.5; n = 21/40), which is interpreted as the crystallization age (Fig.4-1c).

4.2.2 Granite (Zg-119)

The sample Zg-119 was sampled from the diamond drill hole (DDH) ZG-20-21 (interval in meters: 555,30m –to- 568,50m), representing the Zgounder Mine exploration program from 2020, and referred to as the ‘Deep Intrusion’ (Mine terminology). On hand, the sample corresponds to a fine to medium-grained light grey granite with pink passes. Zircon grains from this sample are homogenous in size, mostly euhedral to subhedral with some rounded zircon grains. CL images show visible oscillatory zoning with local moderately fractured zircons showing dark overgrowths (Fig. 4-2a). The discordance filter used for this sample was the same as for Zg-106; thus, zircons falling outside 95% to 105% concordance were omitted from the age calculation. A total of high-quality zircon analyses yielded a reliable concordia age of 564 ± 2 Ma (MSWD = 1.6; n = 34/37). We also calculated a weighted mean age using a broader selection of concordant zircons within error, which gave an equivalent age of 564 ± 2 Ma (MSWD = 1.1; n = 76/160) (Fig. 4-2b). However, the zircon U-Pb are quite complicated and seem to spread over ~80 Ma which is likely due to the combined effects of Pb loss and inheritance (Fig. 4. 2-b). Hence both were omitted from the age calculation. We interpret the youngest tail of ages (~ 520 Ma) which are clearly outside of the main population reflecting analysis that have been affected by Pb loss (Sharman and Malkowski, 2024). Whilst oldest zircons are probably inherited (~ 620 Ma), and referring to a detrital signature. However, the analyzed detrital sample (Zg-132), that represents the sedimentary succession in which this granite is intruded has no zircons of this age (see supplementary table 5 for Zg-132). Moreover, the inheritance signature cannot be supported as no xenocrystic zircons were observed in the CL images. Overall, as both ages are statistically identical, we interpret the 564 ± 2 Ma as the robust crystallization age for the granite (Fig. 4-2c).

https://doi.org/10.5194/egusphere-2025-6178
Preprint. Discussion started: 18 December 2025

4.2.3 Sandstone (Zg-132)

This sample was collected from the Ag-Hg hosting sedimentary units from the Imghi Formation of Saghro Group near the Zgounder Mine entrance (Fig. 2). It is a fine to medium-grained greenish sandstone. On the outcrop, it follows the E-W-trending direction of the Imghi Formation, dipping at 70° to the south. For Thomas et al., (2002), the Imghi Formation represents the lower thick beds of greywacke/turbiditic section of Saghro Group, and seems to represent a typical flysch succession, which is interpreted as the primary sedimentary fill of a back-arc basin associated with the Khzama ophiolite complex. Most zircons from this sample are uniformly rounded and fragmented. They are distinguishable by their low CL signal with some being preferentially zoned (Fig. 4-3a). The age calculation utilized a filtered dataset, specifically incorporating only zircons that fell within the 95% to 105% concordance range. A total of 139 analyses were obtained on zircons from this sample, of which 91 are concordant (Fig. 4-3b). The ages distribution is dominated by one single population. For the detrital zircons, one uniform peak at around 2100 Ma, with one zircon recording an age at 3700 Ma (Fig. 4-3c).

https://doi.org/10.5194/egusphere-2025-6178
Preprint. Discussion started: 18 December 2025

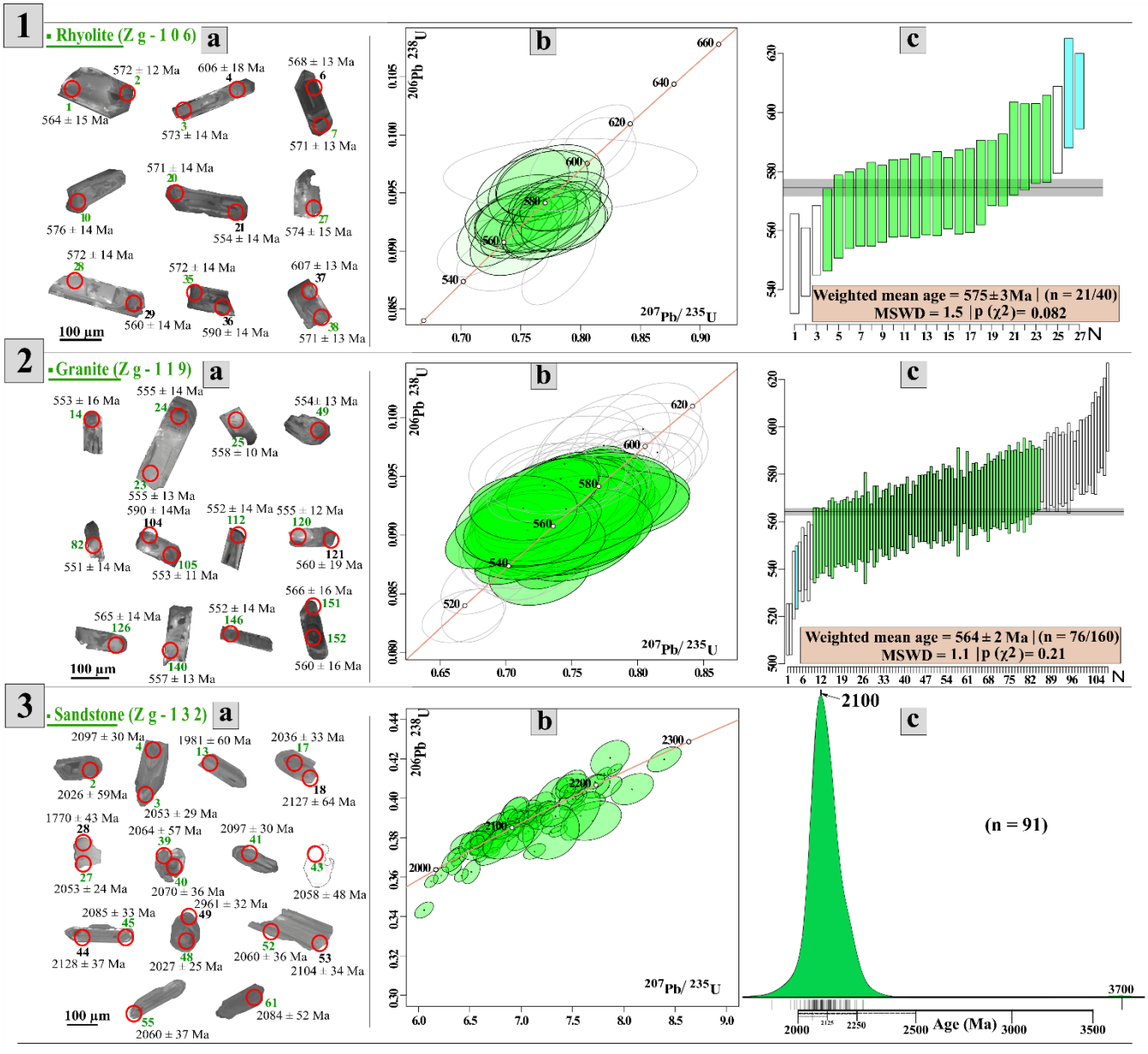

Figure 4: Cathodoluminescence (CL) images for selected zircons, U-Pb concordia and Pb^{206} / U^{238} weighted mean diagrams for samples (1) Zg-106 (rhyolite), and (2) Zg-119 (granite); along with U-Pb concordia diagram and KDE for (3) Zg-132 (sandstone). Error ellipses are plotted at 2σ. Ages were calculated using Isoplot R 1.0 (Vermeesch, 2018).

4.3 Whole-rock geochemistry

Due to samples distribution and geological diversity, the selected samples are organized in respect to their lithostratigraphic position, and hence treated accordingly. The whole-rock data for 32 samples are listed in supplementary table 4. For a start, we assessed the behavior of mobile elements and how it relates with the formed alteration minerals, using the diagram of Large

https://doi.org/10.5194/egusphere-2025-6178
Preprint. Discussion started: 18 December 2025

et al., (2001); and samples are plotted in (Fig. 5). The rock material loss of ignition (LOI) at 1100 °C is low for most samples (less than 2 wt. %), except for the mafic and intermediate terms of Saghro Group where it is close to 4 wt. % (e.g. basalt, gabbro and andesite samples). On plotting our data in this diagram, a homogenous hydrothermal trend is clearly defined for all samples except for sample (Zg-106). Its trend is more directed towards sericite alteration, typical of a distal ore environment (Large et al., 2001). Overall, the plot confirms that most of our samples plot in the domain of '''Least altered rocks'''.

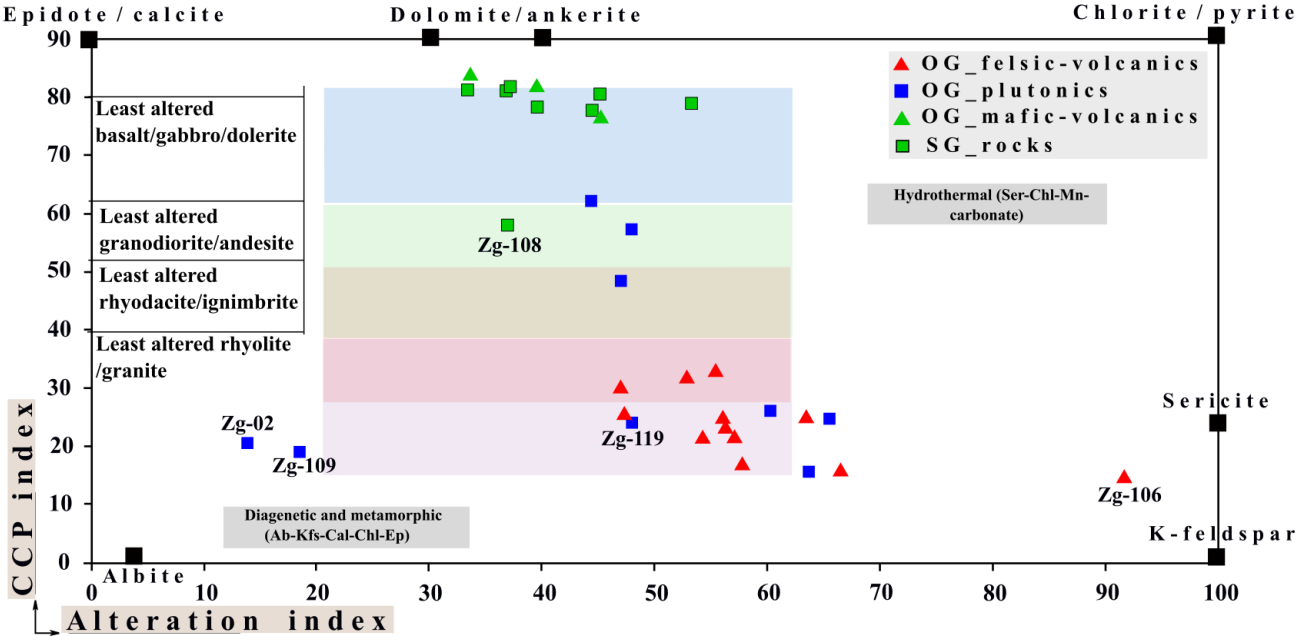

Figure 5: Plots of the studied rocks on the alteration box diagram (Large et al., 2001). Alteration Index (AI) = 100 x (K_2O + MgO) / (K_2O + MgO + Na_2O + CaO), Chlorite-carbonate-pyrite index (CCPI) = 100 x (MgO + FeO) / (MgO + FeO + Na_2O + K_2O).

4.3.1 The Saghro Group rocks

The analyzed Saghro Group rocks belong to the Tittalt Formation of the Saghro Group in the study area (Fig. 1C; Fig. 2; Thomas et al., 2002, 2004). Geochemically, they define a narrow range of compositions, with SiO_2 contents from 48.85 wt.% to 52.87 wt.%, except for sample (Zg-108) with SiO_2 of 61.15 wt.%. They contain 1.08 – 7.45 wt.% MgO; 13.44 – 15.65 wt.% Al_2O_3; 2.82 – 3.95 wt.%, Na_2O and 0.47 – 3.07 wt.% K_2O. Based on the Nb/Y vs Zr/TiO_2 diagram (Fig. 6a), except for one sample (Zg-108) with andesitic composition, all samples plot within a sub-alkaline basalt; similar to contemporaneous mafic-intermediate rocks from the Saghro (Errami et al., 2009) and Sirwa inliers (Thomas et al., 2002). Most rocks are metaluminous except for one sample (Zg-006) which is peraluminous (Fig. 6b). In addition, the Saghro Group rocks display a calc-alkaline signature (Fig. 6c).

Using rare earth elements (REE) (Fig. 6d), the Saghro Group samples show a total REE varying between 60.94 to 231.77 ppm with coherent patterns characterized by a slight LREEs enrichments and HREE depletion with $(La/Yb)_N$ ratios ranging from 1.83 to 6.42. Almost all samples have slight/no important negative Eu anomalies (δEu = 0.88–0.98) to less positive anomaly

https://doi.org/10.5194/egusphere-2025-6178
Preprint. Discussion started: 18 December 2025

for one sample of gabbro (Zg-105; Eu/Eu*)N = 1.28; Fig. 6d). For the multi-elements diagram (Fig. 6e), the Saghro Group rocks exhibit an enrichment of large ion lithophile elements (LILE, like Rb, Ba, K) over high field strength elements (HFSE) with negative anomalies in Nb, Ta, and a prominent positive Pb anomaly. They do compare in the most part with basaltic rocks from the Saghro Group of Kelâat M'gouna inlier (Benziane et al., 2008; Fekkak et al., 2001), and the early gabbro sample from Sirwa (Touil et al., 2008; Fig. 6d).

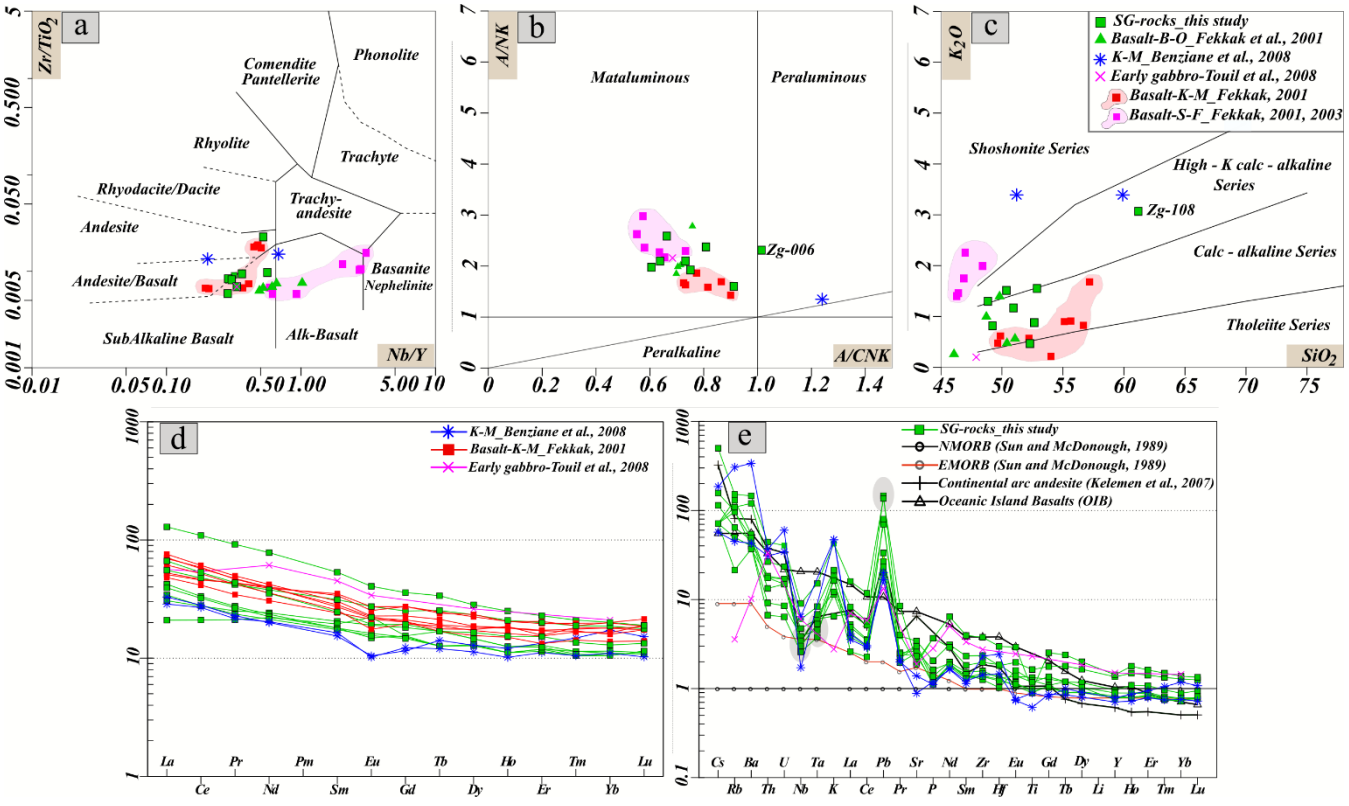

Figure 6: Saghro Group:(a) Nb/Y versus Zr/TiO_2 (Winchester and Floyd, 1977). (b) Plot of A/NK vs. A/CNK [A/CNK = molar ratio Al_2O_3 / ($CaO + Na_2O + K_2O$) and A/NK = molar ratio Al2O3 / ($Na_2O + K_2O$)](Shand, 1943). (c) K_2O versus SiO_2. (d) Chondrite-normalized REE diagram of Boynton, (1984). (e) NMORB normalized diagram; normalization values are sourced from Sun and McDonough, (1989). SG samples are plotted against reference rocks from the literature. Abbreviations: B-O : Boumalne; K-M: Kelâat M'gouna; S-F: Sidi Flah.

4.3.2 The Ouarzazate Group rocks

The studied samples representing the Ouarzazate Group are composed of both volcanic and plutonic rocks. The felsic volcanic and plutonic samples have high contents in SiO_2 (79.89 – 61.16 wt.%), Al_2O_3 (15.18 – 10.83 wt.%), and CaO (4.42 – 0.1 wt.%) and low MgO (2.83 – 0.06 wt.%), Ni (60 - 20 ppm) and Co content (19 - 1 ppm), except for one granite (Zg-119) that have relatively high Co content of 109 ppm. Moreover, they have a $Na_2O + K_2O$ = 8.97 to 6.31 with a K_2O/Na_2O ratio of 20.75 to 0.14. Rock types for felsic volcanics are as follows: ignimbrites are represented as rhyodacite and dacite, while rhyolites and rhyolitic-ignimbrites plot inside the rhyolite field (Fig. 7a). Furthermore, the plutonic rocks occupy the granite field, with three

https://doi.org/10.5194/egusphere-2025-6178
Preprint. Discussion started: 18 December 2025

distinctive granodiorites (not shown). The whole set consist of high-K calc-alkaline to shoshonitic rocks (Fig. 7b), and are peraluminous, except for the granodiorite samples that exhibit a metaluminous character (Fig. 7c). Overall, all samples plot within the calc-alkaline and alkali-calcic slightly migrating towards alkaline field (Fig.7d).

Mafic volcanics (e.g. dolerite) have moderate SiO_2 contents of (51.56 – 50.58 wt.%), Al_2O_3 (14.69 – 13.9 wt.%), moderate CaO (7.67 – 5.61 wt.%) and moderate MgO (5.3 – 4.56 wt.%). K_2O/Na_2O ratio values are 0.73 to 0.26, along with Na_2O+K_2O ratio = 5.64 to 3.58 (supplementary table 4). They are sub-alkaline basalts (Fig. 7a), with a calc-alkaline signature (Fig. 7b), and a metaluminous character (Fig. 7c).

In the REE diagram (Fig. 7e), all felsic volcanic and plutonic samples show homogeneous patterns, with enriched LREEs over HREEs. $(La/Yb)_N$ ratio varies between 17.93 and 2.1, except for one rhyolitic sample Zg-106 with $(La/Yb)_N$ of 0.89. All samples have high Eu negative anomaly (Eu/Eu* = 0.61 – 0.34, except for the same Zg-106 sample, that exhibits a prominent Eu anomaly with Eu/Eu* = 0.04, controlled by advanced plagioclase crystallization. In the multi-element spider diagram, all samples display enrichments in LILEs (Cs, Rb, Ba, Th, and U) and depletion in HFSEs (Zr, Nb, Hf and Ta), relative to Primitive Mantle (Fig. 7f). Plus, samples show a prominent negative anomaly in Nb, Ta, P and Ti along a positive anomaly in Pb, Ba and Th, except for sample Zg-106 that lacks negative Nb anomaly.

For the mafic volcanics, the REE normalized to chondrite (Fig. 7e) show moderate LREE enrichments over HREE with less fractional patterns ($(La/Yb)_N$ = 6.22 to 5.94) and very low/absent Eu anomaly (Eu/Eu* = 0.98 to 0.88). However, our dolerites are distinguished by their homogenous pattern with a prominent Pb enrichment, with less significant Sr anomaly (Fig. 7f). Our dolerites resemble those of the Tifnout Valley (TV), Group A and B, and Zaghar mafic dikes from the Sirwa massif by Belkacim et al., (2017); Touil et al., (1999); Toummite et al., (2013), respectively. Even so, minor differences related to prominent negative Nb and Ti anomaly are observed for reference samples compared to our dolerites' positive Ti anomaly (Fig. 7f). However, they differ from the Bas Drâa inlier mafic-intermediate bodies, which lack Pb enrichment and Sr depletion Karaoui et al., (2014).

https://doi.org/10.5194/egusphere-2025-6178
Preprint. Discussion started: 18 December 2025

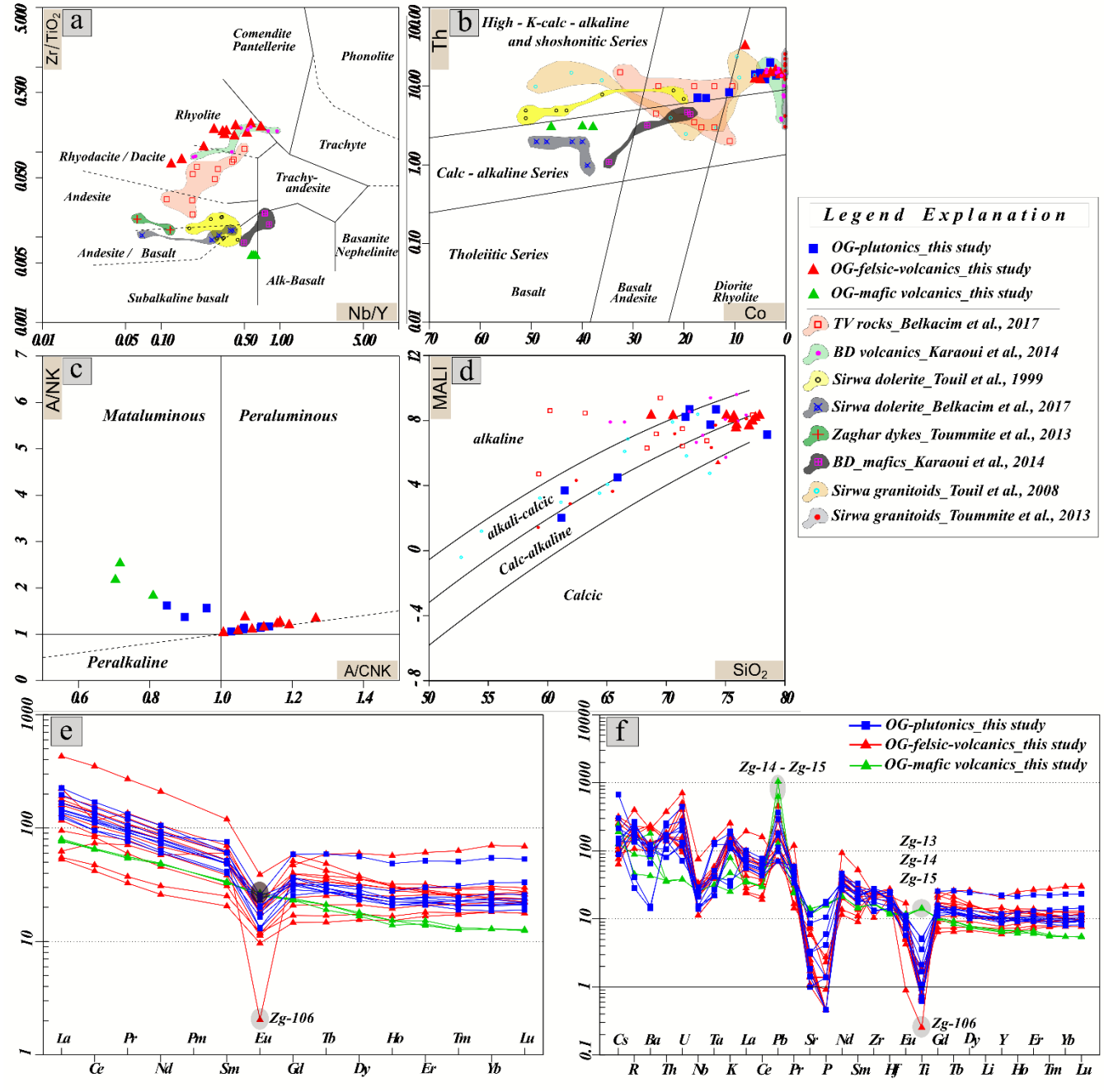

Figure 7: Ouarzazate Group: (a) Nb/Y versus Zr/TiO_2 (Winchester and Floyd, 1977). (b) Th vs Co plot of Hastie et al., (2007). (c) Plot of A/NK vs. A/CNK of Shand, (1943). (d) MALI diagram of Frost et al., (2001). (e) Chondrite-normalized REE diagram of Boynton, (1984). (f) Primitive mantle normalized diagram of Sun and McDonough, (1989). OG samples are plotted against reference rocks from the literature. Abbreviations: TV: Tifnoute Valley; BD: Bas Draâ.

https://doi.org/10.5194/egusphere-2025-6178
Preprint. Discussion started: 18 December 2025

4.4 Significance of Sm-Nd isotopic data

Sm-Nd isotopic studies of seven representative samples covering the Ediacaran record of the Sirwa massif reveal petrogenesis processes and orogenic evolution between the 630 to 538 Ma evolution of the Anti-Atlas belt post-Bou Azzer-Sirwa ophiolite accretion. Results are listed in table 2.

Lithology	Sample code	Sm (ppm)	Nd (ppm)	147Sm/144Nd	143Nd/144Nd	± 2 SE	ƐNd(0)	ƐNd(570)	TDM (Goldstein) Ma	TDM Ga
Ouarzazate Group rocks										
Granodiorite	Zg-09	10.23	50.70	0.1220	0.512414	0.000005	- 4,4	+ 1,1	1252,8	1,24
Dolerite	Zg-14	6.518	28.99	0.1359	0.512390	0.000010	- 4,8	- 0,4	1526,7	1,51
Rhyolite	Zg-106	11.50	32.75	0.2124	0.512693	0.000007	+ 1,1	- 0,1	0	N/A
Rhyolite	Zg-117	10.69	50.59	0.1278	0.512332	0.000011	- 6,0	- 0,9	1483,7	1,47
Granite	Zg-119	9.106	42.92	0.1283	0.512381	0.000009	- 5,0	0,0	1404,8	1,39
Saghro Group rocks										
Gabbro	Zg-105	3.739	13.27	0.1704	0.512762	0.000011	+ 2,4	+ 4,5	1431,6	N/A
Andesite	Zg-108	8.943	40.03	0.1351	0.512550	0.000007	- 1,7	+ 3,2	1197,3	1,19

Table 2: Sm-Nd isotopic data for the analyzed Saghro Group and Ouarzazate Group rocks. TDM is the Depleted Mantle Age in Ga calculated using the linear model of Goldstein et al., (1984); and is not calculated for samples with 147Sm/144Nd ratios greater than 0.145 (e.g. Zg-106, Zg-105). Abbreviations: ± 2 SE: Standard Errors (Uncertainty in Nd isotopic composition); N/A : Not Available.

Based on field relationships, An angular unconformity (Errami et al., 2009; Thomas et al., 2002), and a significant sedimentary/magmatic gap exist between the 630 - 600 Ma Saghro Group and the overlaying 570 - 538 Ma Ouarzazate Group (Errami et al., 2021a). We have used the 620 Ma as a reference age for εNd analyses of Saghro Group samples (Zg-105, and Zg-108). They show narrow (^{143}Nd /^{144}Nd) 620 Ma ratios, from 0.512001 to 0.512070, and positive εNd (at 620 Ma) values between + 3.2 to + 4.5. Additionally, the TDM model ages (Fig. 8a), ranging from 1431 – 1197 Ma, exceed the individual maximum depositional ages of 630 to 600 Ma, and the crystallization ages of pre to contemporaneous igneous intrusions found elsewhere in the Anti-Atlas belt that fall within the bracket of 640 Ma to 580 Ma, respectively (Errami et al., 2021a; O'Connor et al., 2010; Liégeois et al., 2006; Gasquet et al., 2005; Mrini, 1993). Overall, the Saghro Group samples show a mixed origin with εNd (620 Ma) ranging from + 3.2 to + 4.5, indicating a blend of mantle-derived magma and moderate contribution of an old crust (Paleoproterozoic ?). This contrasts the basaltic rocks studied in the Saghro region by Errami et al., (2009), for which εNd (at 640 Ma) vary between + 7.63 to + 8.08, suggesting a juvenile source, with no Paleoproterozoic influence. Consequently, authors argued that the Saghro Group's sedimentary and volcanic deposits attest to an active back-arc basin, with the arc itself located north of the Saghro mountains in the Saghro inlier (Errami et al., 2009).

Ouarzazate Group rocks exhibit a mostly uniform distribution with ($^{143}Nd/^{144}Nd$) 570 Ma values from 0.511855 to 0.511958. These ratios are close to or slightly lower than the Chondritic Uniform Reservoir (CHUR) values. Moreover, for all samples, the εNd570 values range from - 0.9 to + 1.1. Volcanic rocks show negative εNd570 values: -0.9 (Tadmant rhyolite), - 0.1 (Ouarzazate Group rhyolite), and - 0.4 (dolerite). Granitoids have εNd570 values of + 0.0 to + 1.1 for Zg-119 and Zg-09, respectively. This range in values suggests mixing or variable degrees of interaction between a mantle source and an older

https://doi.org/10.5194/egusphere-2025-6178
Preprint. Discussion started: 18 December 2025

crustal component. In addition, the TDM model ages for all of these samples range from 1526 to 1252 Ma (Fig. 8c), indicating a Mesoproterozoic affinity, even though the effect is limited. Admitting that Mesoproterozoic rocks are scarce to absent in the Anti-Atlas, these Proterozoic TDM ages, in conjunction with the mixed (near zero) εNd (570 Ma) values for both volcanic and plutonic rocks, strongly suggest that the magma for the Ouarzazate Group are likely to represent mixed values involving a Pan-African juvenile mantle together with moderate but discernible contribution from an older crustal material of Mesoproterozoic in age, which itself incorporated some even older (Paleoproterozoic ?) material (Baidada et al., 2017; El Bahat et al., 2017; Blein et al., 2014b; Gasquet et al., 2005; Thomas et al., 2002) (Fig. 8d). All in all, these results do confirm the presence of an old cratonic basement beneath the Central Anti-Atlas.

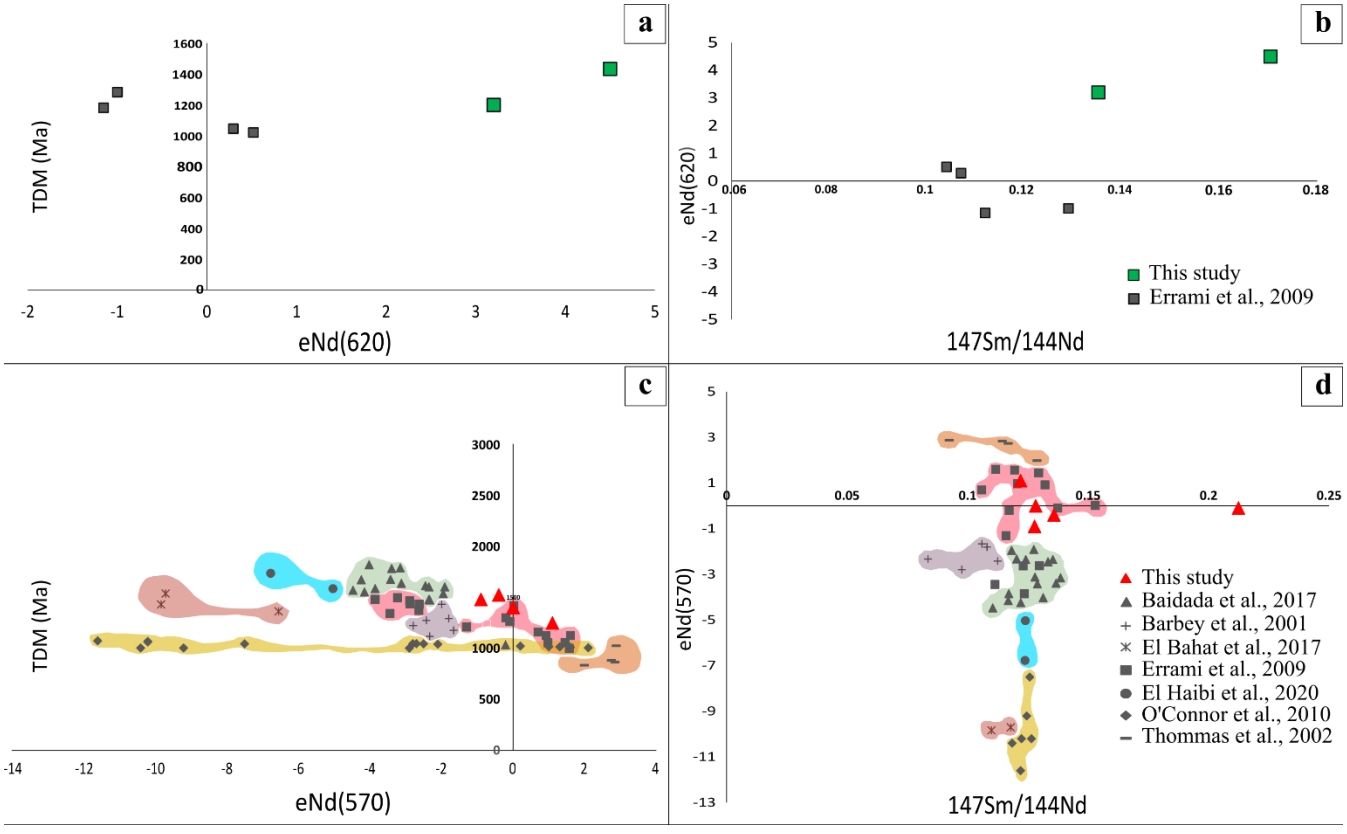

Figure 8: (a) εNd_{620} vs TDM model ages for SG. (b) εNd_{620} vs $^{147}Sm/^{144}Nd$ diagram for SG. (c) εNd_{570} vs TDM model ages for OG. (d) εNd_{570} vs $^{147}Sm/^{144}Nd$ diagram for OG rocks. All samples are compared with selected and available reference rocks from the literature.

https://doi.org/10.5194/egusphere-2025-6178
Preprint. Discussion started: 18 December 2025

5 Discussions

5.1 Petrogenesis

5.1.1 The Saghro Group rocks

The Saghro Group rocks consist of basaltic lava flows interbedded with marine, low-grade metasediments. The geochemical fingerprint of the mafic rocks is well-suited for investigating the orogenic processes involved in magma genesis (Pearce, 1983; Wood, 1980). However, it is crucial to evaluate the effects of alteration, metamorphism, and crustal contamination before exploring the magmatic evolution.

- **Alteration effect**

The analyzed samples exhibit loss on ignition (LOI) values of 2 to 4 wt.%, implying major elements and LILE mobility during alteration process (supplementary table 4). Saghro Group basalt samples display scattered large-ion lithophile elements (LILEs; e.g., K, Rb, Na, Sr, Pb) vs. Zr, suggesting alteration variances. In contrast, binary plots of high-field-strength elements (HFSEs; e.g., Nb, Ta, Ti, Hf) and rare earth elements (REEs) against Zr exhibit consistent linear trends, reflecting their immobile nature (Pearce, 1996; supplementary table 4). All samples from this Group are classified as minimally altered basalts (Large et al., 2001) (Fig. 5).

- **Fractional crystallization and crustal contamination**

The analyzed samples predominantly consist of basalts displaying negative correlations for Al_2O_3, CaO, MgO, Fe_2O_3, and TiO_2 vs. Zr, and a positive correlation for P_2O_5, indicating fractional crystallization during magma evolution. The Mg# values (12.13 to 43.26), reflect early fractionation of ferromagnesian minerals, and suggest that the Saghro Group samples are not derived from a primitive melt. Furthermore, the absence of a significant Eu anomaly ($\delta Eu = 0.88–1.28$) indicates limited plagioclase fractionation (Fig. 6d). The lack of a negative Eu anomaly, despite the evolved nature of the magmas (low Mg#), is likely due to the mixing of evolved basaltic magmas (low Mg#), with more primitive magmas that lacked plagioclase fractionation.

In a contamination-sensitive trace element diagram (Th/Ce and Th/La) (Fig. 9a), our samples show ratios of 0.047 to 0.080 and 0.115 to 0.172, respectively. The trend suggest that crustal contamination played a significant role in magma genesis (Taylor and McLennan, 1995). Additionally, the low Ce/Pb ratio (~ 4.3) further highlights continental crustal influence (Hofmann et al., 1986; supplementary table 4 for calculation). Further, a binary mixing model with Nd isotopic data (supplementary table 4 for calculation; De Paolo, 1981), interprets the Saghro Group basalts as formed from the mixing of a magmatic melt contaminated by 17 – 18% Paleoproterozoic continental crust ($\varepsilon Nd620 = -16$; Ennih and Liégeois, 2008) and 82 – 83% primitive mantle ($\varepsilon Nd620 = +8$; Errami et al., 2009). This is further supported by the negative correlation of εNd values with SiO_2, and relatively low εNd values (+ 3.2 to + 4.5), compared to contemporary mantle-derived Saghro inlier basalts ($\varepsilon Nd = +8$; Errami et al., 2009).

However, the observed enrichment may stem from either continental crust contamination or mantle source enrichment. The Th/Ce and Th/La ratios for our samples plot linearly near the MORB reservoir, far from the upper continental crust (UCC)

https://doi.org/10.5194/egusphere-2025-6178
Preprint. Discussion started: 18 December 2025

field, suggesting limited direct crustal input (Fig. 9a). Moreover, ratios such as (Sm/Yb)N versus (Nb/La)N (Safonova et al., 2016), sensitive to the nature of the mantle source, range from 1.64 to 2.74 and 0.50 to 0.91, respectively. These values place the Saghro Group samples in a transitional domain between MORB and IAB, closer to the field of back-arc basalts (BAB) (Fig. 9b). Similarly, Th/Nb and Ta/Nd ratios (0.12 – 0.30 and 0.03 – 0.06, respectively) indicate a transitional composition between MORB and the mafic lower continental crust (MLCC) (Aldanmaz et al., 2008; Fig. 9c), in alignment with the source diagram (Laurent et al., 2014; Fig. 9d), where all the Saghro Group rocks derived from fractional crystallization and contamination/assimilation of primary mafic lithologies straddling the boundary between high-K to low-K mafic rocks. Overall, the Saghro Group samples originate from the melting of an enriched source transitional between MORB and IAB, followed by fractional crystallization involving ferromagnesian minerals and assimilation of lower Paleoproterozoic continental crust.

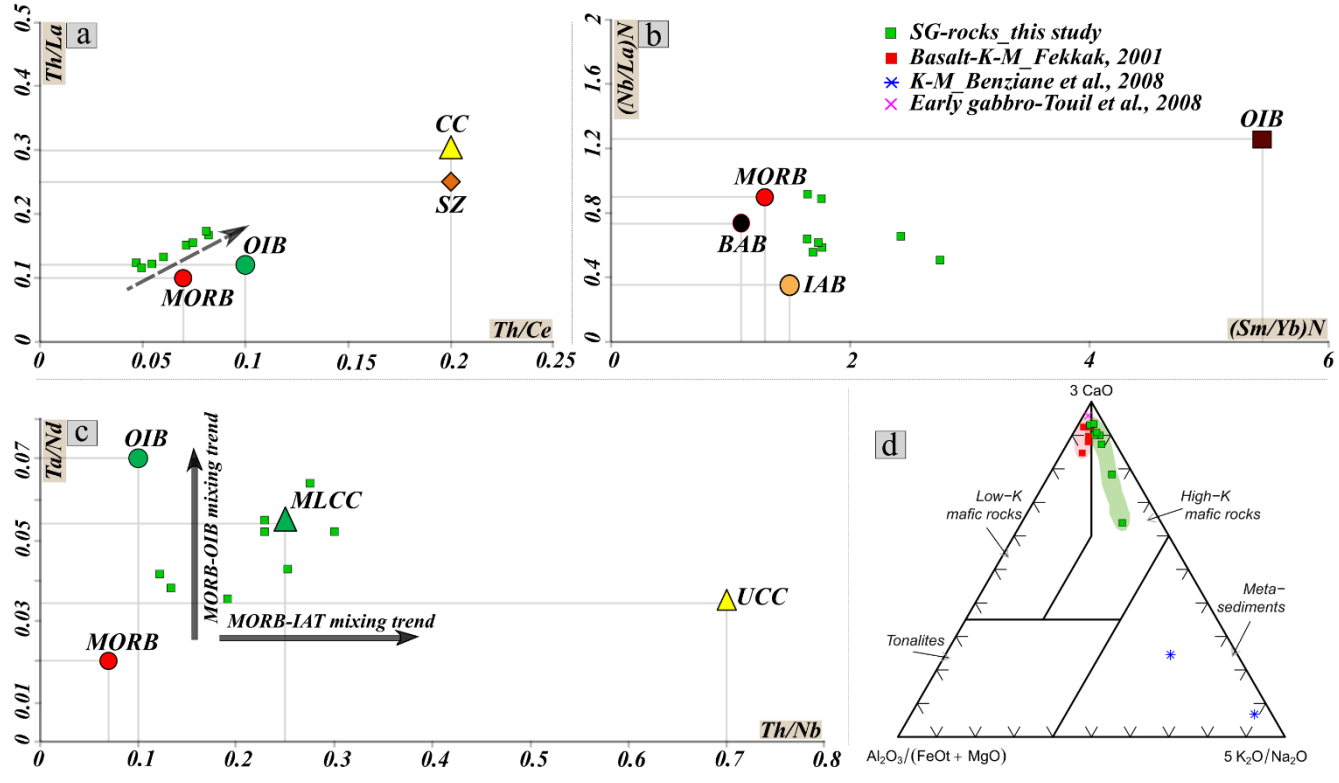

Figure 9: Saghro Group: (a) Th/Ce vs Th/La ratios for SG (Taylor and Mc Lennan, 1995). (b) plot of (Sm/Yb)N vs (Nb/La)N (Safonova et al., 2016). (c) Th/Nb vs Ta/Nd plot (Aldanmaz et al., 2008). (d) The source diagram of Laurent et al., (2014). Abbreviations: K-M: Kelâat M'gouna.

5.1.2 The Ouarzazate Group rocks

- **Fractional crystallization and crustal contamination**

https://doi.org/10.5194/egusphere-2025-6178
Preprint. Discussion started: 18 December 2025

The Ouarzazate Group's volcanic and plutonic rocks exhibit chemical evolution that can be explained by fractional crystallization, with decreasing Al2O3, Fe2O3, MgO, CaO, TiO2, and P2O5 vs. rising SiO2. Major elements vs. Zr show no significant correlations (not shown: see supplementary table 4). Selected trace elements, such as Sr, decrease with rising SiO2, typical of plagioclase crystallization. Interestingly, Some trace elements (e.g. Cr, Ni, Ba, Rb, Zr) show disruptions in their patterns with increasing SiO2. Ni uniformly declines then sharply increases, Cr rises steadily then increases, while Ba, Zr, and Rb rise then decline, particularly at 70 wt.% SiO2 (Fig. 10a). These patterns are likely due to a magma recharge event affecting pre-magma's crystallization (Fig. 10a).

Felsic volcanics and plutonics compensate for Sr and P depletion due to plagioclase and apatite fractionation (Fig. 7f). A prominent negative Eu anomaly in rhyolite Zg-106 indicates early calcic phase crystallization, while the absence of an Eu anomaly in dolerites suggests limited plagioclase involvement (Fig. 7e). Additionally, their Pb enrichment indicates crust assimilation (Fig. 7f). The high La (16.4 to 133 ppm) and Ce (33.8 to 284 ppm) values in the Ouarzazate Group samples suggest interaction between parental magma (s) and crust material, indicating enrichment due to either assimilation of continental crust or a combination of assimilation and fractional crystallization during magma ascent (De Paolo, 1981). Further, fractional crystallization relates to correlations between Zr and Th/Nb ratios (Fig. 10b), as most of the Ouarzazate Group felsic volcanics and plutonics show similar Th/Nb and Zr trends, indicating significant assimilation and fractional crystallization in magma evolution. Some plutonics, however, show a limited Th/Nb range, suggesting bulk assimilation control (Fig. 10b). This is supported by the La/Sm versus La diagram (Fig. 10c) indicating source heterogeneity, despite fractional crystallization's dominance. The Y/Nb versus SiO2 wt.% (Fig. 10d) confirms a crustal source with varying differentiation. Depletions in P, Nb, and Ti in Ouarzazate Group rocks (Fig. 7f) suggest crustal contamination and hydrous metasomatism, with P anomalies linked to Nb and Ti depletions (Campbell et al., 1994). In addition, the depletion of HFSEs like Nb and Ti might also indicate magmatic arc signatures and possible crustal contamination during magma processes (Wilson, 1989). All samples show slight K enrichments (Fig. 7f), likely related to fluids from subducted sediments (Beraaouz et al., 2004).

https://doi.org/10.5194/egusphere-2025-6178
Preprint. Discussion started: 18 December 2025

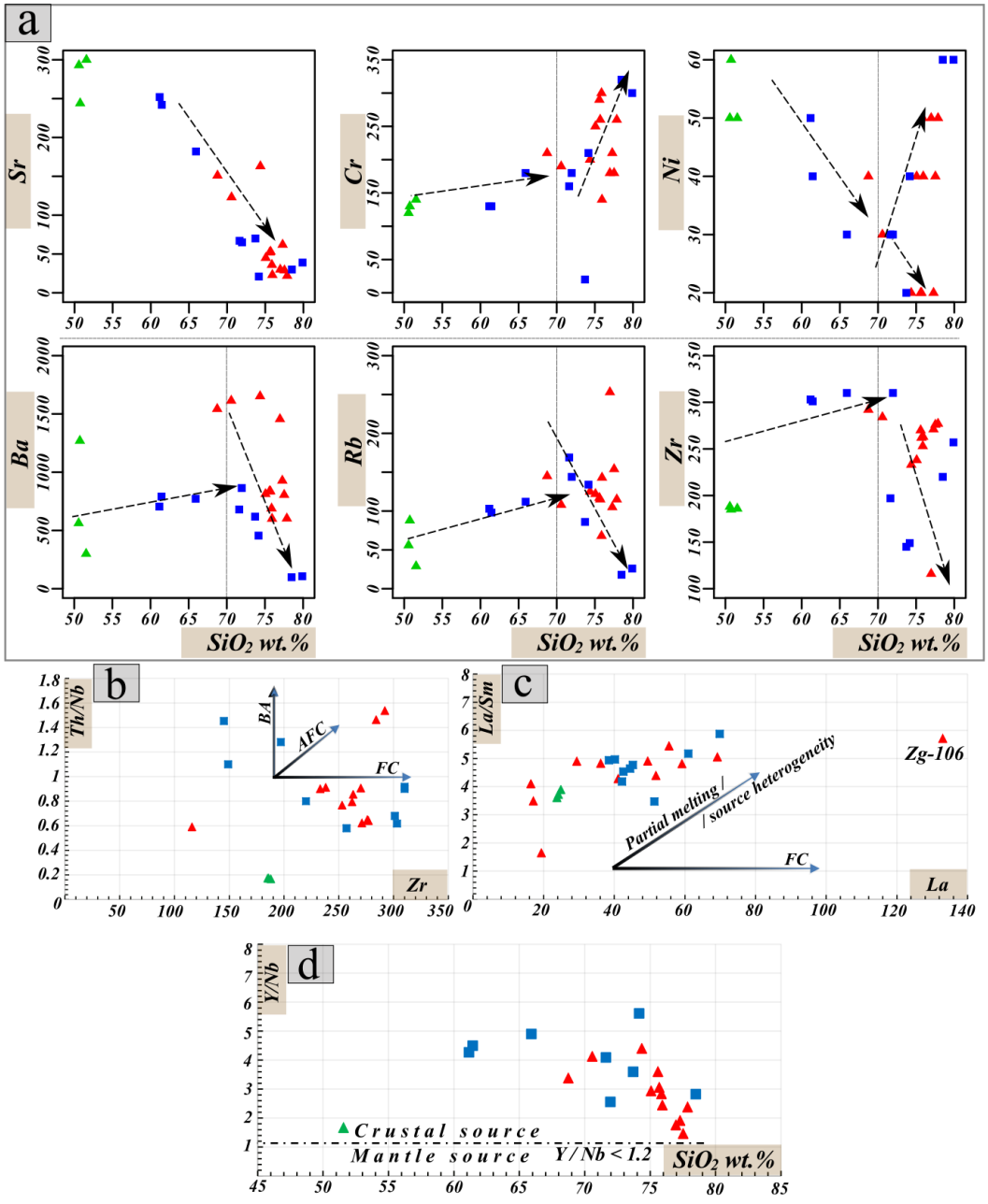

435

Figure 10: Ouarzazate Group: (a) Harker variation diagrams for selected trace elements (e.g. Sr, Cr, Ni, Ba, Rb, Zr) for the OG rocks. (b) plot of Th/Nb vs Zr. (c) La/Sm vs La plot. (d) Y/Nb vs increasing SiO_2, (Eby, 1990) for the Y/Nb =1.2 discriminating value. Abbreviations: BA: Bulk Assimilation; AFC: Assimilation and Fractional Crystallization; FC: Fractional Crystallization.

- **Magma types and source characteristics**

440 The coherent negative anomalies in Nb, P, and Ti in the Ouarzazate Group samples might suggest an exclusive crustal origin, with minor discrepancies due to advanced degrees of differentiation. These features may also arise from low partial melting

https://doi.org/10.5194/egusphere-2025-6178
Preprint. Discussion started: 18 December 2025

of metasomatized mantle contaminated by continental material (O'Reilly and Griffin, 2013), as supported by εNd values (- 0.9 to + 1.1) indicating juvenile magma contributions. Indeed, trace elements and isotopic compositions can clarify subduction input versus crustal contamination. The Ouarzazate Group rocks show significant LILE and LREE enrichment with Nb-Ta depletion, indicating a metasomatized lithospheric mantle from subduction or assimilation of enriched continental crust (Fig. 7-f). Furthermore, the Th/Yb versus Ta/Yb diagram suggests that the magma source originated from an E-MORB-type mantle, evolving through contamination and Assimilation-Fractional Crystallization, as evidenced by the trend of the samples toward the average upper continental crust (Fig. 12a). This interpretation is consistent with the moderate εNd values and TDM ages that reflect contributions from both mantle and continental crustal components, highlighting the importance of crustal contribution over sediment zone enrichment (Fig. 12b). All in all, the primary magma responsible for the genesis of the Ouarzazate Group rocks sourced from an enriched continental lithospheric mantle, previously underwent metasomatism by fluids from former Neoproterozoic subduction.

5.2 Geodynamic implications and regional correlations

5.2.1 The Saghro Group

Previously, the Saghro Group basin was interpreted as consisting of distal deep marine sediments equivalent to the platform series of Tachdamt Group, formed during the initial rifting associated with the Rodinia breakup (Thomas et al., 2002). However, recent zircon data from the Saghro Group sediments in the Sirwa and Saghro inliers suggest its deposition, post the Bou Azzer–Sirwa ophiolite accretion, during the main Pan-African orogeny (Abati et al., 2010; Errami et al., 2009; Liégeois et al., 2006).

Basaltic samples from the Sirwa inlier (this study) show enrichment in large ion lithophile elements (LILE) and light rare earth elements (LREE) relative to high field strength elements (HFSE) and heavy rare earth elements (HREE). They also exhibit pronounced negative anomalies in Nb, Ta, and Ti, suggesting a subduction zone fluids influence (Wilson, 1989). Despite this, the basalts feature high Zr and relatively low Y concentrations, classifying them as within-plate basalts (WPB) (Fig. 11a). This dual geochemical signature, blending within-plate and active margin characteristics, is further evidenced by their Ti/Y and Zr/Y ratios which plot in transitional field in the geotectonic discrimination diagram (Ti/Y versus Zr/Y; Pearce and Gale, (1977), not shown). Indeed, the coexistence of geotectonic signatures from both active continental margins and within-plate settings is characteristic of magmas generated during back-arc extension (Shinjo and Kato, 2000).

In this context, the subduction-related signature is acquired through mantle metasomatism by sediment/fluid-derived components during arc activity, while the within-plate signature emerges later during back-arc extension processes. This interpretation aligns with the geochemical characteristics of the Saghro Group basalts, which plot within the fields of mid-ocean ridge basalt (MORB) and back-arc basin basalt (BABB) (Fig. 11b). Moreover, the active margin signature is supported by high Th/Nb and low U/Th ratios in the Saghro Group basalts (refer to supplementary table 4). Further, the influence of

https://doi.org/10.5194/egusphere-2025-6178
Preprint. Discussion started: 18 December 2025

subduction-related components is further highlighted by the ThN vs NbN ratios, with the basalts plotting above the MORB-OIB array (Fig. 11c). This pattern indicates a mantle source enriched during continental arc processes (Pearce, 1983).

At a regional scale, basaltic flows have been described as interbedded within the sediments of the Saghro Group in the Saghro massif (Errami et al., 2009; Fekkak et al., 2003, 2001). They exhibit diverse geochemical signatures. For a start, the basalts in Sidi Flah (SF) are of Initial Rift Tholeiites (IRT) and Ocean Island Basalts (OIB) character, while those from the Kelâat M'gouna (KM) inlier are Nb-depleted. In contrast, the Anou N'Izem basalts in the Boumalne (BO) inlier possess typical Mid-Ocean Ridge Basalt (MORB) signatures. U-Pb dating of detrital zircons from the Saghro Group in various inliers suggests that this unit was deposited between 640 - 600 Ma across the entire Central-Eastern Anti-Atlas region (Errami et al., 2021a; Abati et al., 2010) (Fig. 13A). This geochemical variation may reflect a single geodynamic event. Specifically, during the evolution of a back-arc basin, the earliest magmas generated often exhibit magmatic arc characteristics due to the proximity of the back-arc to the arc itself. As the back-arc basin evolves and the magma source becomes further removed from the metasomatised mantle, the magmas acquire within-plate geochemical signatures (Vasey et al., 2021; Saunders and Tarney, 1984). Overall, basaltic magmatism in the Saghro Group fits this evolutionary framework. For instance, calc-alkaline basalts from the Sirwa inlier (Thomas et al., 2002; This study), reflect initial stages in back-arc formation. Conversely, and higher in the stratigraphy; IRT, OIB, and MORB-type basalts indicate later stages in back-arc evolution. This interpretation is consistent with sediment geochemistry suggesting back-arc basin deposition (Ouguir et al., 1996). Furthermore, this scenario aligns with the paleogeographic position of the Anti-Atlas during the Ediacaran. During that time, the Anti-Atlas region was dissected in a northward direction (present coordinates) due to south-dipping Cadomian subduction (Fig. 13) (Rojo-Pérez et al., 2024; Stern, 2024; Errami et al., 2021a; Linneman et al., 2014).

https://doi.org/10.5194/egusphere-2025-6178
Preprint. Discussion started: 18 December 2025

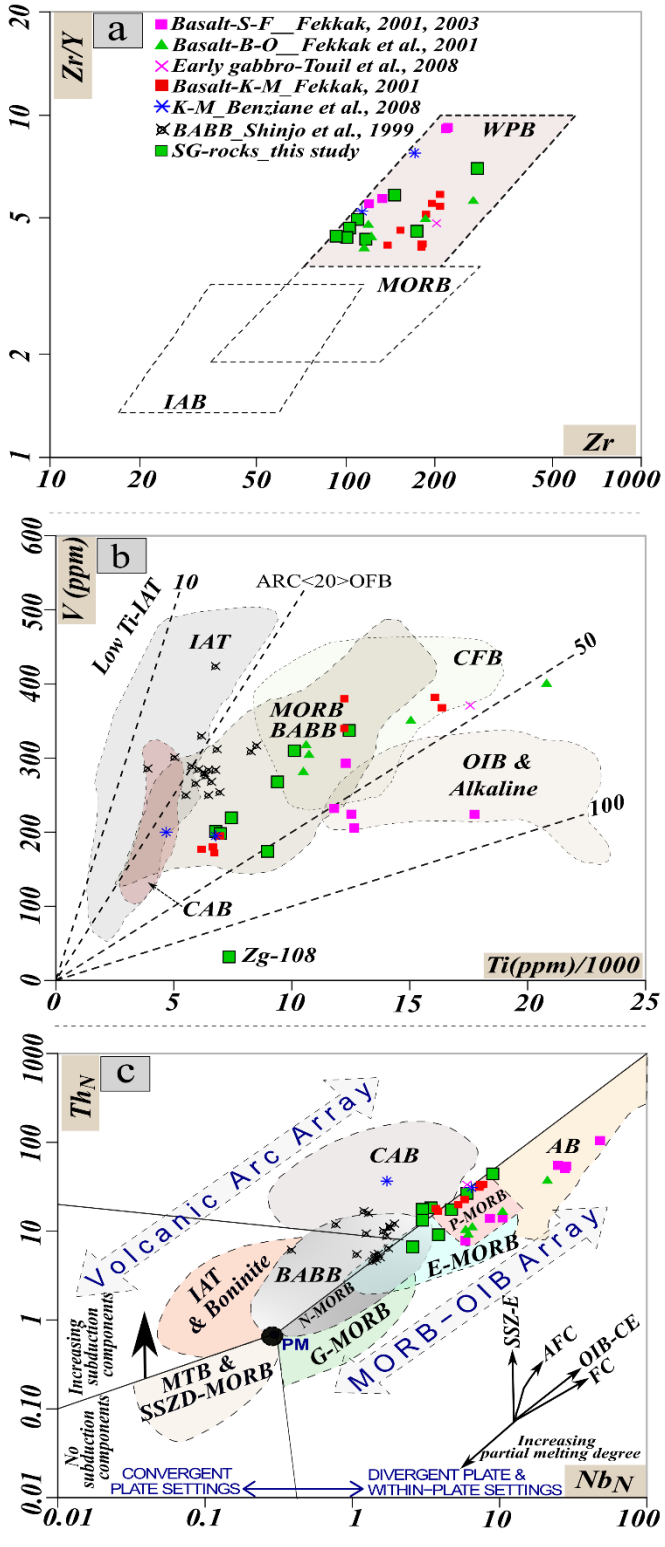

https://doi.org/10.5194/egusphere-2025-6178
Preprint. Discussion started: 18 December 2025

Figure 11: Saghro Group: (a) Zr/Y vs Zr plot for basalts of SG (Pearce and Norry, 1979). (b) V vs Ti/1000 plot (Shervais, 1982). (c) plot of Th_N vs Nb_N ratios (Saccani, 2015). Abbreviations: B-O : Boumalne; K-M: Kelâat M'gouna; S-F: Sidi Flah; BABB: Back-arc basin basalts.

5.2.2 The Ouarzazate Group

On the tectonic discrimination diagrams (Fig. 12b-c), the Ouarzazate Group rocks display geochemical characteristics ranging from dominating within-plate to minor active continental margins (oceanic island arcs). Plus, the high Th/Yb ratios > 1 for all rocks refer to a metasomatised mantle source in subduction zone and/or crustal contamination. All in all, the whole accounts for a post-collisional setting (Fig. 12c), involving partial melting of a pre-existing lithospheric source, either a mantle or crust. Hence, controlling the recharge in K_2O and LILE (e.g. Rb, Ba) contents for the majority of our samples (Fig. 11a). Additionally, the alkali-calcic to high-K calc-alkaline signature of our samples is in fact typical to post-collisional events (Liégeois et al., 1998, and reference therein).

The Ediacaran magmatism of the Ouarzazate Group is still debated as being fully post-collisional and linked to asthenospheric rise (upwelling) beneath the WAC during its metacratonic evolution (Belkacim et al., 2017; Gasquet et al., 2008, 2005; Liégeois et al., 2006; Thomas et al., 2002), or related to subduction (Walsh et al., 2012; Benziane, 2007; El Baghdadi et al., 2003), or even representing the Iapetus Ocean opening with ties to the Ediacaran Central Iapetus Magmatic Province (CIMP; Youbi et al., 2020). Nonetheless, subduction-related features can arise in a non-subduction settings without coeval subduction (Morris et al., 2000; M'arquez et al., 1999; Cousens, 1996; Hooper et al., 1995).

Regional correlations with similar magmatism lead us to attribute the Ouarzazate Group to a post-collisional event also exemplified in numerous inliers of the Anti-Atlas (Fig. 13C-D) (Yajioui et al., 2020; Karaoui et al., 2015; Linneman et al., 2014; Toummite et al., 2013; Walsh et al., 2012; Gasquet et al., 2005, 2004; Thomas et al., 2002).

https://doi.org/10.5194/egusphere-2025-6178
Preprint. Discussion started: 18 December 2025

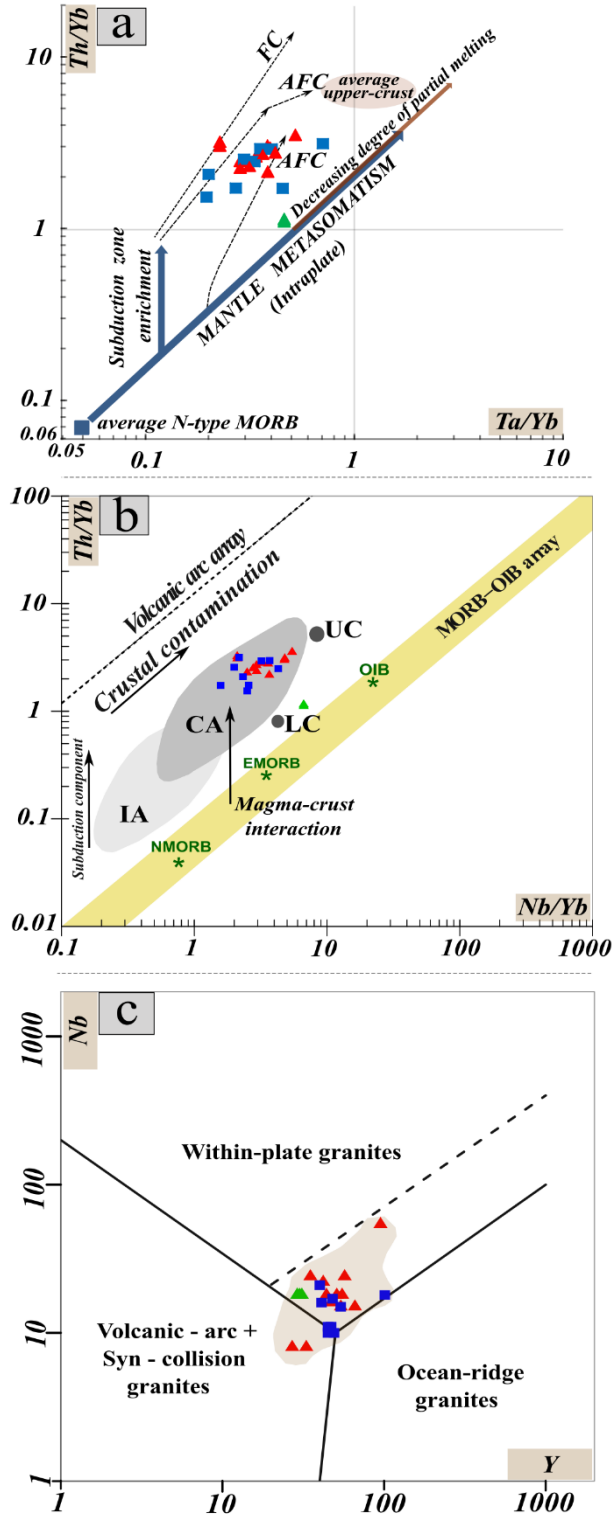

https://doi.org/10.5194/egusphere-2025-6178
Preprint. Discussion started: 18 December 2025

Figure 12: (a) Th/Yb vs Ta/Yb plot for OG rocks. (b) Nb/Yb vs Th/Yb diagram of Pearce, (2008). (c) Nb versus Y diagram (Pearce et al., 1984) depicting evolution from volcanic arc granite to within-plate granite.

5.3 Significance of LA-ICP-MS U-Pb data

5.3.1 U-Pb zircon age record on magmatic rocks of the OG

Reliable new U-Pb zircon ages on two magmatic samples (Zg-106, and Zg-119; Fig. 4), representing the Ouarzazate Group from the Sirwa massif returned ages of 575 ± 3 Ma and the 564 ± 2 Ma, respectively. These ages are consistent with a lower Ouarzazate Group affinity, and represent the extension of the Ediacaran magmatism previously described in numerous inliers of the Anti-Atlas belt (Yajioui et al., 2020; Karaoui et al., 2015; Hefferan et al., 2014, and references therein; Toummite et al., 2013; Walsh et al., 2012; Gasquet et al., 2005, 2004; Thomas et al., 2002).

Indeed, in the Zgounder Mine Region, similar volcanic activity of this type can be bracketed between 620 Ma to 550 Ma (Pelleter et al., 2016; Thomas et al., 2002; This study). For the rhyolite (Zg-106); Pelleter et al., (2016) reported mean age of 578 ± 4 Ma from the Zgounder Mine for the rhyolitic dikes and plugs using the 207Pb/206Pb ages. Moreover, in the Sirwa massif, similar U–Pb ages of 579 ± 7 Ma, 571 ± 8 Ma, 577 ± 6 Ma, 579 ± 7, and 575 ± 8 Ma were proposed for the Tourcht diorite, the Tikhfist rhyolite (Tiouin Subgroup, Fig. 1C), the Aguins member (Tafrant Subgroup), the Tilsakht granite, and the Askaoun granodiorite, respectively (Thomas et al., 2002). Given that the 575 ± 3 Ma age of our rhyolite is analytically identical within errors to the ages of these rocks, thus inferring a rapid sequence of intrusive events that occurred within a span of a few million years.

For the granite sample (Zg-119); the obtained age of 564 ± 2 Ma is also identical within a margin of error to the ages of the neighbouring Imourkhssen granite dated respectively at 561 ± 3 Ma, and 562 ± 5 Ma by Toummite et al., (2013), and Thomas et al., (2002) (Fig. 1C). The Imourkhssen granite on its turn intrudes the lower and older part of the Ouarzazate Group in the Sirwa massif (Thomas et al., 2002). Additionally, in the Sirwa massif, numerous syn- to late-Ouarzazate Group granites with a sub-alkaline-calcic composition provided ages of c. 560 Ma, making them the Ouarzazate Group's youngest components. According to Thomas et al., (2002), these granites belong to the Achkoukchi Complex (Fig. 1C), and grouped into the Amassine Suite (e.g., Bou-Tazart, Aït Nabdas, and Tikitar granites, and the Tazoult Quartz-porphyry at 559 ± 6 Ma).

Significant inherited Paleoproterozoic zircon population are previously reported for the Ouarzazate Group rocks all over the Anti-Atlas. For instance, Baidada et al., (2019) reported inherited Paleoproterozoic signature for the Saghro massif granitoids. Blein et al., 2014b proved the existence of Paleoproterozoic inherited zircon in ignimbrite of the Ouarzazate Group in the Agadir Melloul area. Finally, Thomas et al., (2002) highlighted Paleoproterozoic inherited zircons in syn-Ouarzazate Group granites in the Sirwa massif.

Indeed, the Ouarzazate Group's thick successions of volcano-sedimentary series are dominated by acidic and intermediate high-K calc-alkaline to shoshonitic volcanism (Blein et al., 2014b; Toummite et al., 2013; Walsh et al., 2012; Gasquet et al., 2008, 2005; Benziane, 2007; Thomas et al., 2004; El Baghdadi et al., 2003). Their depositional environment as pull-apart basins with strike-slip faulting conditions and sub-vertical movements favored a high variability in thickness (Walsh et al.,

https://doi.org/10.5194/egusphere-2025-6178
Preprint. Discussion started: 18 December 2025

2012, and references therein). Nevertheless, a contemporaneous magmatic activity spanned the 630 to 538 Ma time frame; (Table 1 in Hefferan et al., (2014) for reported precision ages from selected inliers of the Anti-Atlas Mountains). All in all, this activity indicates a prolonged tectono-magmatic event emplaced over multiple pulses over the whole Anti-Atlas belt (Tuduri et al., 2018). In regard to this, Schulte et al., (2022), considered the Ouarzazate Group in the Central and Eastern Anti-Atlas as the relicts of an Ediacaran silicic large igneous province (SLIP) deposited in a strictly continental environment. These huge volumes of mostly felsic magma were emplaced by multiple pulses and occur as a result of a long-lived magmatic event evolving from high-K calc-alkaline at 575–550 Ma to alkaline affinity at 550–540 Ma (Schulte et al., 2022; Blein et al., 2014b; Gasquet et al., 2008). This magmatism is considered to belong to a continental silicic large igneous province (SLIP), referred to as the Ouarzazate Silicic Large Igneous Province (OSLIP), and emplaced over multiple periods at ca. 575 Ma, ca. 560 Ma, and ca. 550 Ma (Tuduri et al., 2018; Blein et al., 2014b). Consequently, the last two pulses at the final stage of the Pan-African orogeny (560 to 550 Ma) appear linked to widespread pervasive hydrothermal activity across the whole Anti-Atlas (Tuduri et al., 2018). Regional correlations can be drawn to the extent of the Cadomian orogeny (Linnemann et al., 2014, and references therein). Hence, our samples fall within the age range of 580 to 550 Ma of the Cadomian arc magmatism extended to Iberia (Chichorro et al., 2022, and references therein).

5.3.2 The Saghro Group detrital age: depositional style and material source

Whether or not the Paleoproterozoic basement exists in the Sirwa massif north of the AAMF, and by consequence the northern margin of the WAC is still debated (Ennih and Liégeois, 2008). Outcrops of this Paleoproterozoic basement have been regarded as being present exclusively in the westernmost part of the Anti-Atlas belt (Choubert, 1963). However, new studies based on TDM ages support the hypothesis that Paleoproterozoic rocks may also be found in both the Central and Eastern segments of the Anti-Atlas (Baidada et al., 2019; Blein et al., 2014; Toummite et al., 2013; Liégeois et al., 2013; Abati et al., 2010; Gasquet et al., 2008; Thomas et al., 2002). Moreover, this hypothesis can be extended to Western Meseta (Pereira et al., 2015, and references therein; Tahiri et al., 2010; Baudin et al., 2003).

During the last decade, the northern boundary of the WAC is considered to be marked by the northernmost outcrops of highly deformed rocks in the southern part of the Bou-Azzer inlier, particularly the Tazagzaout migmatites and gneisses, based on similarities in lithology and deformation degree with the Zenaga Complex in the Western Anti-Atlas (Leblanc and Lancelot, 1980). However, this view has been changed owing to the new U-Pb precision dating obtained from the Tazagzaout gneisses ($752 \pm {}^{1}{}_{2}$ Ma; D'Lemos et al., (2006), and the Oumlil granite 741 ± 9 Ma; El Hadi et al., (2010)). Furthermore, the positive Nd values of (+ 4.9 to + 6) for the Tazagzaout Complex refer to a juvenile depleted mantle source, not akin to the 2 Ga Eburnean WAC basement (D'Lemos et al., 2006). Consequently, the presence of a WAC basement beneath the Central Anti-Atlas, especially in the Sirwa massif is not clear. Published geochronological data indicate that both the Saghro and Bou Salda groups were deposited approximately 630 to 610 Ma. This deposition occurred during a period of tectonic convergence of the Cadomian arc upon the WAC Iriri-Tazagzaout Complex (Errami et al., 2021a; Walsh et al., 2012; El Hadi et al., 2010). Yet, the precise location of the suture zone marking this collision remains ambiguous. Current interpretations suggest the suture

https://doi.org/10.5194/egusphere-2025-6178
Preprint. Discussion started: 18 December 2025

likely corresponds to the Anti-Atlas Major Fault (AAMF) (Hefferan et al., 2014), potentially extending north along the South Atlas Fault (SAF) (Ennih and Liégeois, 2001, 2008).

Detrital zircon age from our study provides new insights into the basement beneath the Sirwa massif. Sample (Zg-132) from the Imghi Formation of the Saghro Group returned exclusively Paleoproterozoic ages, with a prominent peak at ca. 2100 Ma (Fig. 4-3). Interestingly, no ages younger than 1600 Ma were found in our sample, nor were any zircons dating to the local Pan-African magmatic period in the Anti-Atlas identified. These 883 - 640 Ma Pan-African younger zircons, which are common in outcrops of the Sirwa inlier and have been consistently reported in Saghro Group sediments (Letsch et al., 2018; Abati et al., 2010) are absent in our sample. Indeed, this Paleoproterozoic peak goes in line with the inherited signature from the analyzed zircon population of sediments of the Saghro and Bou Salda groups from the Sirwa massif, for which the obtained maximum depositional ages cluster around 620 – 610 Ma (Abati et al., 2010). Arguably, the authors argued in favor of an exposure of cratonic basement (Paleoproterozoic ?) based on the relatively high proportion of the 610 Ma zircons in regard to Paleoproterozoic zircons in the upper levels of the stratigraphy sequence. Therefore, this suggests that the source of the 610 Ma was eroded favoring the enrichment in Paleoproterozoic ages. Admittedly, the subsequent erosion of the underlying Neoproterozoic rocks (notably synchronous magmatic rocks, and Saghro and Bou Salda groups) might be the source for the prominent 610 Ma peak in the Iberian massif (Chichorro et al., 2022); (Fig. 13A).

The mono-peak at 2.1 Ga can only be accepted to strictly represent Paleoproterozoic. It can be interpreted as representing the material source for the Saghro Group sedimentary units only in the study area (Fig. 13A). Indeed, the returned mono zircon population may reflect insufficient sampling of detrital zircons. However, the number of analyzed zircons (up to 139; see supplementary table 5) is considered adequate to address paleogeographic questions and sediment source areas. In this context, we interpret the Paleoproterozoic mono-peak in our sample to reflect local exposure of Paleoproterozoic basement rocks along the basin margins of the Saghro Group in the study area (Fig. 13A). Consequently, most sediments were derived exclusively from the erosion of these basement rocks in a possible mono Paleoproterozoic paleo-relief without interaction with Cryogenian sediments.

Overall, this evidence argues that during Ediacaran times, the Paleoproterozoic basement was in fact totally or locally exposed in the Sirwa inlier (Fig. 13A). This interpretation is further corroborated by Nd model ages of Ediacaran magmatism from this study (see section Sm-Nd), which yield TDM age of Mesoproterozoic values, indicating a mixing/recycling of older Paleoproterozoic crust with juvenile Ediacaran magma. All in all, and based on these findings, the WAC crust extends beneath the Sirwa massif and likely continues northward far beyond the Anti-Atlas belt. Notably, Paleoproterozoic rhyolites have been reported in the Meseta Block, north of the Anti-Atlas, with a given age of 2050.6 ± 3 Ma (Pereira et al., 2015). These findings do support the extension of the WAC Paleoproterozoic crust northward beyond the AAMF, which was previously considered the northern margin of the craton.

https://doi.org/10.5194/egusphere-2025-6178
Preprint. Discussion started: 18 December 2025

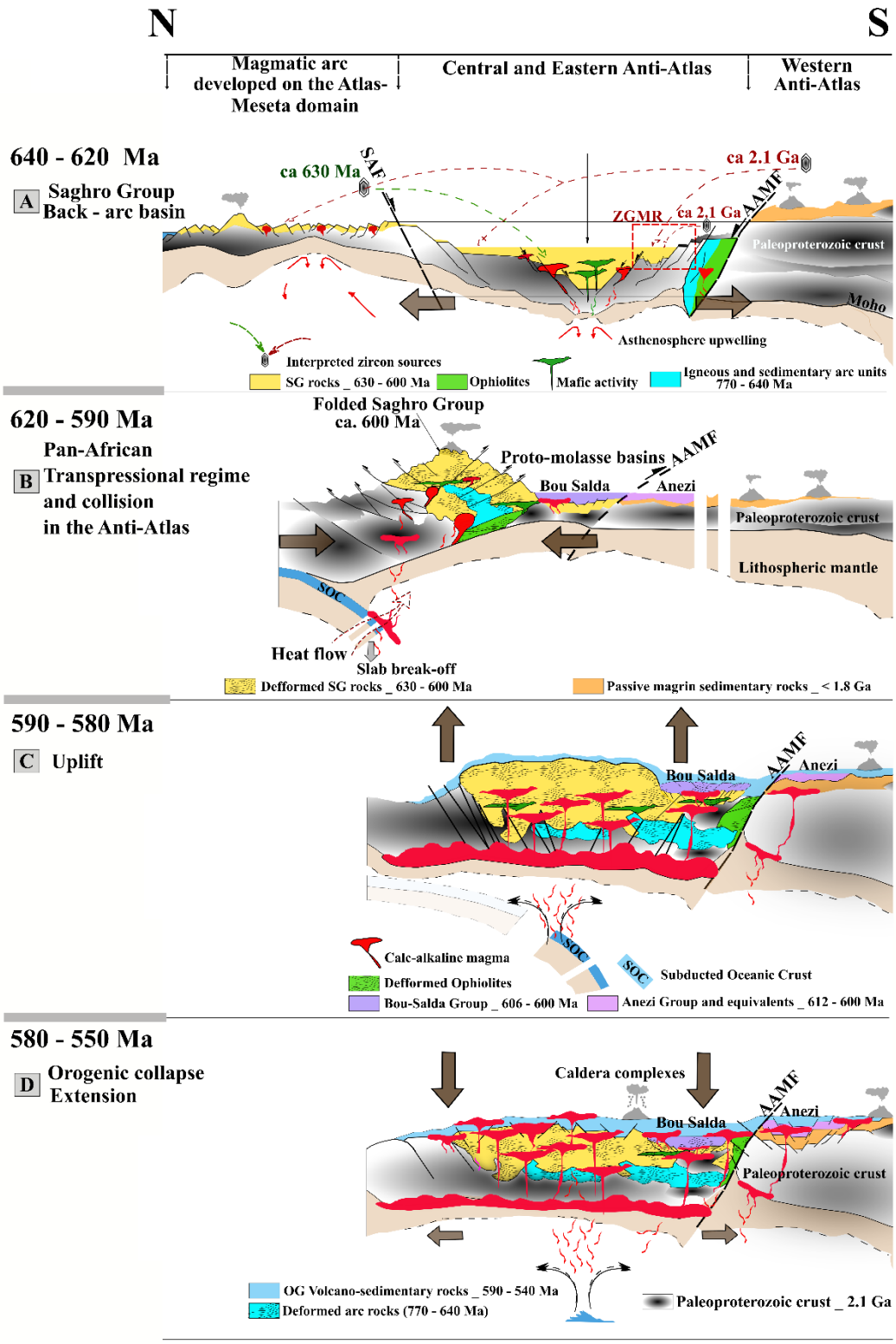

https://doi.org/10.5194/egusphere-2025-6178
Preprint. Discussion started: 18 December 2025

Figure 13: Reconstruction of the geotectonic setting of Saghro Group and Ouarzazate Group during Ediacaran times. (resembled and modified after El Kabouri et al., 2025; Chichorro et al., 2022; Errami et al., 2021a; Abati et al., 2010; Thomas et al., 2002). (A): Saghro Group deposition in a back-arc basin (This study; Ouguir et al., 1996), implying local exposure of the 2.1 Ga Paleoproterozoic crust in the Zgounder Mine Region (This study). (B): Pan-African transpressional regime and collision in the Anti-Atlas, resulting in Saghro Group folding, injection of the 600 Ma calc-alkaline magma (Errami et al., 2021a), and proto molasses basin formation (Thomas et al., 2002). (C): General uplift in the Anti-Atlas. (D): Orogenic collapse favoring the thick Ouarzazate Group sedimentation (e.g. post-tectonic molasse deposition and calc-alkaline magmatism, with coeval acidic rocks).

6 Conclusions

In the light of the above, the following conclusions can be drawn:

i. Based on geochemical proxies (major and trace elements), the Saghro Group rocks exhibit both active continental margins and within-plate characteristics. A dual signature characteristic of magmas generated during back-arc extension. Therefore, the recognized subduction-related signature on our samples is acquired through mantle metasomatism by sediment-derived components during arc activity, while the within-plate signature emerges later during back-arc extension processes.

ii. The Saghro Group rocks were emplaced at the early stages of back-arc basin opening, testified by their calc-alkaline affinity, geochemical characteristics and regional correlations. They were derived from contaminated mantle source with an old continental crust. Further, their εNd (at 620 Ma) = + 3.2 to + 4.5, and TDM ages of 1431 – 1197 Ma reflects a mixed origin, combining mostly mantle-derived magma with limited proportion of older crustal material. Thus admitting the existence of an old Paleoproterozoic to even Mesoproterozoic crust under the Saghro Group.

iii. For the Ouarzazate Group rocks, the evolution in chemical compositions for the suite of high-K calc-alkaline to shoshonitic rocks is controlled in the most part by fractional crystallization and crustal contamination. They were deposited in a post-collisional setting, and their primary magma was sourced from an enriched continental lithospheric mantle, previously underwent metasomatism by fluids from former Neoproterozoic subduction. Further, their εNd (at 570 Ma) = - 0.9 to + 1.1, and TDM ages of 1526 to 1252 Ma refer to a Mesoproterozoic (and Paleoproterozoic) affinity, implying recycling of Paleoproterozoic material during Ediacaran times.

iv. LA-ICP-MS U-Pb zircon ages on magmatic rocks evince an expression of a post-collisional syn-orogenic magmatism (WACadomian arc), during the emplacement of its first and second pulses at ca. 575 to 560 Ma. This period of magmatism is concordant with a Silicic Large Igneous Province (SLIP) recognized all over the Anti-Atlas.

Code, data, or code and data availability

Data will be made available upon request.

https://doi.org/10.5194/egusphere-2025-6178
Preprint. Discussion started: 18 December 2025

Supplement link

Author contributions

Abdelhay Ben-Tami: Field work, Sampling and preparation, Thin-sections preparation, Investigation, Data visualization, Data curation, Formal analysis, Writing of original draft, Finalization. **Said Belkacim:** Supervision, Resources, Writing - review and editing. **Jamal El Kabouri:** Data visualization, Writing of original draft. Review and editing. **Joshua H.F.L. Davies and Morgann G. Perrot:** LA-ICP-MS U-Pb data and methodology, writing of original draft, review and editing. **Mariam Ferraq**: Data curation and visualization. **Mohamed Bouabdellah:** review and editing. **Bouchra Baidada, Mohamed Bhilisse** and **Mohamed Assalmi:** Resources, accommodation, field trips, hosting. **David Lalonde:** Resources, Financing, Collaboration. Review, and validation.

Competing interests

The authors declare that they have no conflict of interest. Corresponding author (Abdelhay Ben-Tami), discloses an employment relationship with the Zgounder Millenium Silver Mining Company (ZMSM).

Disclaimer

Copernicus Publications remains neutral with regard to jurisdictional claims made in the text, published maps, institutional affiliations, or any other geographical representation in this paper. While Copernicus Publications makes every effort to include appropriate place names, the final responsibility lies with the authors. Views expressed in the text are those of the authors and do not necessarily reflect the views of the publisher.

Acknowledgements

This research represents a component of the corresponding author's thesis project. The authors express their sincere gratitude to the **Zgounder Millenium Silver Mining Company (ZMSM)**, the Moroccan subsidiary of **Aya Gold and Silver (AYA)**, for their essential financial support for this study, as well as for providing accommodation and logistical assistance. Special appreciation is extended to the Exploration geology team at the Zgounder Mine for their valuable facilitation and support during field operations. Official permission to publish this work was granted by **David Lalonde, P. Geo / VP Exploration / Aya Gold and Silver Inc.** Finally, the authors wish to thank the anonymous referees for their constructive feedback and suggestions, which significantly enhanced the quality of this manuscript.

https://doi.org/10.5194/egusphere-2025-6178
Preprint. Discussion started: 18 December 2025

Financial support

Financial support for the Whole-rock analysis, Sm-Nd isotopes, U-Pb on zircon, fieldwork and accommodation was guaranteed by the **Zgounder Millenium Silver Mining company (ZMSM)**; the Moroccan branch of **Aya Gold and Silver Inc**.

Review statement

References

Abati, J., Aghzer, A. M., Gerdes, A., & Ennih, N.: Detrital zircon ages of Neoproterozoic sequences of the Moroccan Anti-Atlas belt. Precambrian Research, 181(1-4), 115–128, https://doi:10.1016/j.precamres.2010.05.018, 2010.

Admou, H., Fekkak, A., Razin, P., Egal, E., Youbi, N., Soulaimani, A., Blein, O., Baudin, T., Chevremont, P.: Carte géologique Maroc (1/50 000), feuille d'Aït Ahmane– Notes et Mémoires Service Géologique Maroc, no. 533, 2012.

Ait Lahna, A., Youbi, N., Tassinari, C.C.G., Basei, M.A.S., Ernst, R.E., Chaib, L., Barzouk, A., Mata, J., G¨artner, A., Admou, H., Boumehdi, M.A., S¨oderlund, U., Bensalah, M.K., Bodinier, J.L., Maacha, L., Bekker, A.: Revised stratigraphic framework for the lower Anti-Atlas supergroup based on U–Pb geochronology of magmatic and detrital zircons (Zenaga and Bou Azzer-El Graara inliers, Anti-Atlas Belt, Morocco). Journal of African Earth Sciences. 171, 103946, https://doi.org/10.1016/j. jafrearsci.2020.103946, 2020.

Aït Malek, A., Gasquet, D., Bertrand, J.M., Leterrier, J. : Géochronologie U-Pb sur zircon de granitoïdes éburnéens et panafricains dans les boutonnières protérozoïques d'Igherm, du Kerdous et du Bas Drâa (Anti-Atlas occidental, Maroc). Comptes. Rendus. l'Académie des Sciences-Series. IIA–Earth and Planetary Science. 327 (12), 819–826, https://doi.org/10.1016/S1251-8050(99)80056-1, 1998.

Aldanmaz, E., Yaliniz, M. K., Guctekin, A., & Goncuoglu, M. C.: Geochemical characteristics of mafic lavas from the Neotethyan ophiolites in western Turkey: implications for heterogeneous source contribution during variable stages of ocean crust generation. Geological Magazine, 145(1), 37-54, https://doi.org/10.1017/S0016756807003986, 2008.

Álvaro, J.J., Benziane, F., Thomas, R., Walsh, G.J., Yazidi, A.: Neoproterozoic–Cambrian stratigraphic framework of the Anti–Atlas and Ouzellagh promontory (High Atlas), Morocco. Journal of African Earth Sciences. 98, 19–33, https://doi.org/10.1016/j.jafrearsci.2014.04.026, 2014.

Álvaro, J. J., Pouclet, A., Ezzouhairi, H., Soulaimani, A., Bouougri, E. H., Imaz, A. G., and Fekkak, A.: Early Neoproterozoic rift-related magmatism in the Anti-Atlas margin of the West African craton, Morocco. Precambrian Research, 255, 433-442, https://doi.org/10.1016/j.precamres.2014.10.008, 2014b.

Baidada, B., Ikenne, M., Barbey, P., Soulaimani, A., Cousens, B., Haissen, F., Ilmen, Said, Alansari, A.: SHRIMP U–Pb zircon geochronology of the granitoids of the Imiter Inlier: constraints on the Pan-African events in the Saghro massif, Anti-Atlas (Morocco). Journal of African Earth Sciences. 150, 799–810, https://doi.org/10.1016/j. jafrearsci.2018.10.008, 2019.

https://doi.org/10.5194/egusphere-2025-6178
Preprint. Discussion started: 18 December 2025

Baidada, B., Cousens, B., Alansari, A., Soulaimani, A., Barbey, P., Ilmen, S., & Ikenne, M.: Geochemistry and Sm–Nd isotopic composition of the Imiter Pan-African granitoids (Saghro massif, eastern Anti-Atlas, Morocco): Geotectonic implications. Journal of African Earth Sciences, 127, 99–112, https://doi:10.1016/j.jafrearsci.2016.08.016, 2017.

Bajja, A.: Volcanisme syn à post orogénique du Néoprotérozoïque de l'Anti-Atlas: implications pétrogénétiques et géodynamiques. In: de Wall H., Greiling R.P. (Eds.), Magmatic Evolution of a Neoproterozoic Island-Arc Syn- to Postorogenic Igneous Activity in the Anti-Atlas (Morocco). Forschunszentrum Jülich Gmbh 45, pp. 9–228, 2001.

Barbey, P., Nachit, H., and Pons, J.: Magma–host interactions during differentiation and emplacement of a shallow-level, zoned granitic pluton (Tarçouate pluton, Morocco): implications for magma emplacement. Lithos, 58(3-4), 125-143, https://doi.org/10.1016/S0024-4937(01)00053-6, 2001.

Baudin, T., Chèvremont, P., Razin, P., Youbi, N., Andries, D., Hœpffner, C., and Tegyey, M.: Carte géologique du Maroc au 1/50 000, feuille de Skhour des Rehamna, Mémoire explicatif. Notes Mémoires Services Géologiques. Maroc, 435, 114, 2003.

Belkacim, S., Gasquet, D., Liégeois, J.-P., Arai, S., Gahlan, H. A., Ahmed, H., Ikenne, M.: The Ediacaran volcanic rocks and associated mafic dykes of the Ouarzazate Group (Anti-Atlas, Morocco): Clinopyroxene composition, whole-rock geochemistry and Sr-Nd isotopes constraints from the Ouzellarh-Siroua salient (Tifnoute valley). Journal of African Earth Sciences, 127, 113–135, https://doi:10.1016/j.jafrearsci.2016.08.002, 2017.

Ben-Tami, A., Belkacim, S., Baidada, B., El Kabouri, J., Assalmi, M., Bhilisse, M., and Bouabdellah, M.: Lithostratigraphy, Whole-Rock, and Sm–Nd Isotopic Data of the Ediacaran Magmatic Rocks from the Zgounder Ag–Hg Deposit (Siroua Massif, Central Anti-Atlas, Morocco). In international conference on Mediterranean Geosciences Union (pp. 167-171). Cham: Springer Nature Switzerland, https://doi.org/10.1007/978-3-031-48758-3_38, 2024.

Benziane, F., Yazidi, A., Saadane, A., Yazidi, M., El Fahssi, A., Stone, B. D., and Ejjaouani, H.: Carte géologique du Maroc au 1/50 000, feuille KELÂAT M'GOUNA–Notice explicative. Notes Mémoires Service Géologique Maroc, 468, 136, 2008.

Benziane, F.: Lithostratigraphie et évolution géodynamique de l'Anti-Atlas (Maroc) du Paléoprotérozoïque au Néoprotérozoïque: exemples de la boutonnière de Tagragra de Tata et du Jbel Saghro. Thèse de doctorat, Université de Savoie CISM, Chambéry, France. 321 pp, 2007.

Beraaouz, E. H., Ikenne, M., Mortaji, A., Madi, A., Lahmam, M., & Gasquet, D.: Neoproterozoic granitoids associated with the Bou-Azzer ophiolitic melange (Anti-Atlas, Morocco): evidence of adakitic magmatism in an arc segment at the NW edge of the West-African craton. Journal of African Earth Sciences, 39(3-5), 285-293, https://doi.org/10.1016/j.jafrearsci.2004.07.040, 2004.

Blein, O., Baudin, T., Chèvremont, P., Soulaimani, A., Admou, H., Gasquet, P., … Gombert, P.: Geochronological constraints on the polycyclic magmatism in the Bou Azzer-El Graara inlier (Central Anti-Atlas Morocco). Journal of African Earth Sciences, 99, 287–306, https://doi:10.1016/j.jafrearsci.2014.04.021, 2014.

Blein, O., Baudin, T., Soulaimani, A., Cocherie, A., Chèvremont, P., Admou, H., … Roger, J.: New geochemical, geochronological and structural constraints on the Ediacaran evolution of the south Sirwa, Agadir-Melloul and Iguerda inliers, Anti-Atlas, Morocco. Journal of African Earth Sciences, 98, 47–71, https://doi:10.1016/j.jafrearsci.2014.06.019, 2014b.

https://doi.org/10.5194/egusphere-2025-6178
Preprint. Discussion started: 18 December 2025

Bouougri, E. H., Aït Lahna, A., Tassinari, CCG., Basei, MAS., Youbi, N., Admou, H., Saquaque, A., Boumehdi, A., Maacha, L.: Time constraints on early Tonian Rifting and Cryogenian Arc terrane-continent convergence along the northern margin of the West African craton: Insights from SHRIMP and LA-ICP-MS zircon geochronology in the Pan-African Anti-Atlas belt (Morocco). Gondwana Research. 85:169-188, https://doi.org/10.1016/j.gr.2020.03.011, 2020.

Boynton, W. V.: Cosmochemistry of the rare earth elements: meteorite studies. In Developments in geochemistry, Elsevier, (Vol. 2), (pp. 63-114), https://doi.org/10.1016/B978-0-444-42148-7.50008-3, 1984.

Chichorro, M., Solá, A. R., Bento dos Santos, T. M., Lains Amaral, J., & Crispim, L.: Cadomian/Pan-African consolidation of the Iberian Massif assessed by its detrital and inherited zircon populations: is the~ 610Ma age peak a persistent Cadomian magmatic inheritance or the key to unravel its Pan-African basement?. Geologica acta, 20, 1-29, https://doi.org/10.1344/GeologicaActa2022.20.15, 2022.

Choubert, G.: Essai de mise au point du problème des "ignimbrites". Bulletin Volcanologique, 25(1), 123-140, https://doi.org/10.1007/BF02596545, 1963.

Cousens, B.L.: Magmatic evolution of Quaternary mafic magmas at Long Valley Caldera and the Devils Postpile, California: effects of crustal contamination on lithospheric mantle-derived magmas. Journal of Geophysics. Res. 101, https://doi.org/10.1029/ 96JB02093, 27 673–27 689, 1996.

De Beer, C.H., Chevallier, L.P., De Kock, G.S., Gresse, P.G., Thomas, R.J.: Notice Explicative de la Carte Géologique du Maroc au 1/50 000 feuille Sirwa. Notes et Mémoires Service Géologique. Maroc 395, 86, 2000.

De Paolo, D.J.: Trace element and isotopic effects of combined wall-rock assimilation and fractional crystallization. Earth and Planetary Science Letters. 53, 189–202, https://doi.org/10.1016/0012-821X(81)90153-9, 1981.

D'Lemos, R. S., Inglis, J. D., and Samson, S. D.: A newly discovered orogenic event in Morocco: Neoproterozoic ages for supposed Eburnean basement of the Bou Azzer inlier, Anti-Atlas Mountains. Precambrian Research, 147(1-2), 65–78, https://doi:10.1016/j.precamres.2006.02.003, 2006.

Eby, G.N.: The A-type granitoids: a review of their occurrence and chemical characteristics and speculations on their petrogenesis. Lithos. 26, 115–134, https://doi.org/10.1016/0024-4937(90)90043-Z, 1990.

El Baghdadi, M., El Boukhari, A., Jouider, A., Benyoucef, A., Nadem, S.: Calc-alkaline arc I-type granitoid associated with S-type granite in the Pan-African belt of eastern Anti-Atlas (Saghro and Ougnat, South Morocco). Gondwana Research. 6 (4), 557–572, https://doi.org/10.1016/S1342-937X(05)71007-8, 2003.

El Bahat, A., Ikenne, M., Cousens, B., Söderlund, U., Ernst, R., Klausen, M. B., and Youbi, N.: New constraints on the geochronology and Sm-Nd isotopic characteristics of Bas-Drâa mafic dykes, Anti-Atlas of Morocco. Journal of African Earth Sciences, 127, 77-87, https://doi.org/10.1016/j.jafrearsci.2016.09.003, 2017.

El Hadi, H., Simancas, J.F., Martínez-Poyatos, D., Azor, A., Tahiri, A., Montero, P., Fanning, C.M., Bea, F., Gonzalez-Lodeiro, F.: Structural and geochronological constraints on the evolution of the Bou Azzer Neoproterozoic ophiolite (Anti-Atlas, Morocco). Precambrian Research. 182 (1–2), 1–14, https://doi.org/10.1016/j. precamres.2010.06.011, 2010.

https://doi.org/10.5194/egusphere-2025-6178
Preprint. Discussion started: 18 December 2025

El Haibi, H., Hadi, H. E., Tahiri, A., Poyatos, D. M., Gasquet, D., Pérez-Cáceres, I., and Mehdioui, S.: Geochronology and isotopic geochemistry of Ediacaran high-K calc-alkaline felsic volcanism: an example of a Moroccan perigondwanan (Avalonian?) remnant in the El Jadida horst (Mazagonia). Journal of African Earth Sciences, 163, 103669, https://doi.org/10.1016/j.jafrearsci.2019.103669, 2020.

El Kabouri, J., Triantafyllou, A., Errami, E., Belkacim, S., Calassou, E., Zouicha, A., and Linnemann, U.: Revising the lithostratigraphic framework of the Ediacaran succession of the Anti-Atlas belt: correlation across the Cadomian domain of the West African Craton. Journal of African Earth Sciences, 105696, https://doi.org/10.1016/j.jafrearsci.2025.105696, 2025.

Ennih, N., and Liégeois, J. P.: The boundaries of the West African craton, with special reference to the basement of the Moroccan metacratonic Anti-Atlas belt. Geological Society, London, Special Publications, 297(1), 1–17, https://doi.org/10.1144/SP297.1, 2008.

Ennih, N., and Liégeois, J.P.: The Moroccan Anti-Atlas: the West African craton passive margin with limited Pan-African activity. Implications for the northern limit of the craton. Precambrian Research. 112 (3–4), 289–302, https://doi.org/10.1016/S0301-9268 (01)00195-4, 2001.

Errami, E., Linnemann, U., Hofmann, M., G¨artner, A., Zieger, J., G¨artner, J., Mende, K., El Kabouri, J., Gasquet, D., Ennih, N.: From pan-african transpression to cadomian transtension at the west african margin: New U-Pb zircon ages from the eastern saghro inlier (anti-atlas, Morocco). Geological Society. Special Publications. 503, 209–233, https://doi.org/10.1144/SP503-2020-105, 2021a.

Errami, E., Bonin, B., Laduron, D., Lasri, L.: Petrology and geodynamic significance of the post-collisional Pan-African magmatism in the Eastern Saghro area (Anti- Atlas, Morocco). Journal of African Earth Sciences. 55 (1–2), 105–124, https://doi.org/10.1016/j. jafrearsci.2009.02.006, 2009.

Fekkak, A., Pouclet, A., & Benharref, M.: The middle Neoproterozoic sidi flah group (Anti-Atlas, Morocco): syn-rift deposition in a Pan-African continent/ocean transition zone. Journal of African Earth Sciences, 37(1-2), 73-87, https://doi.org/10.1016/S0899-5362(03)00049-6, 2003.

Fekkak, A., Pouclet, A., Ouguir, H., Ouazzani, H., Badra, L., Gasquet, D.: Géochimie et signification géotectonique des volcanites du Cryogénien inférieur du Saghro (Anti-Atlas oriental, Maroc) /Geochemistry and geotectonic significance of Early Cryogenian volcanics of Saghro (Eastern Anti-Atlas, Morocco). Geodinamica. Acta, 14 (6), 373–385, https://doi.org/10.1080/09853111.2001.10510730, 2001.

Frost, B. R., Barnes, C. G., Collins, W. J., Arculus, R. J., Ellis, D. J., and Frost, C. D.: A geochemical classification for granitic rocks. Journal of petrology, 42(11), 2033-2048, https://doi.org/10.1093/petrology/42.11.2033, 2001.

Garfunkel, Z.: The relations between Gondwana and the adjacent peripheral Cadomian domain—constrains on the origin, history, and paleogeography of the peripheral domain. Gondwana Research, 28(4), 1257-1281, https://doi.org/10.1016/j.gr.2015.05.011, 2015.

https://doi.org/10.5194/egusphere-2025-6178
Preprint. Discussion started: 18 December 2025

Gasquet, D., Ennih, N., Liégeois, J.P., Soulaimani, A., Michard, A.: The Pan-African Belt. In: Michard, A., Saddiqi, O., Chalouan, A., Frizon de Lamotte, D. (Eds.), Continental evolution: the geology of Morocco. Lect. Notes Earth Sci. 116, 33–64, https://doi.org/10.1007/978-3-540-77076-3_2, 2008.

Gasquet, D., Levresse, G., Cheilletz, A., Azizi-Samir, M. R., and Mouttaqi, A.: Contribution to a geodynamic reconstruction of the Anti-Atlas (Morocco) during Pan-African times with the emphasis on inversion tectonics and metallogenic activity at the Precambrian–Cambrian transition. Precambrian Research, 140(3-4), 157–182, https://doi:10.1016/j.precamres.2005.06.009, 2005.

Gasquet, D., Chevremont, P., Baudin, T., Chalot-Prat, F., Guerrot, C., Cocherie, A., and Cheilletz, A.: Polycyclic magmatism in the tagragra d'akka and kerdous–tafeltast inliers (western Anti-Atlas, Morocco). Journal of African Earth Sciences, 39(3-5), 267-275, https://doi.org/10.1016/j.jafrearsci.2004.07.062, 2004.

Goldstein, S. L., O'nions, R. K., and Hamilton, P. J.: A Sm-Nd isotopic study of atmospheric dusts and particulates from major river systems. Earth and planetary Science letters, 70(2), 221-236, https://doi.org/10.1016/0012-821X(84)90007-4, 1984.

Gresse, P.G., De Beer, C.H., Chevallier, L.P., De Kock, G.S., Thomas, R.J. : Notice Explicative de la Carte Géologique du Maroc au 1/50 000 feuille Tachoukacht. Notes et Mémoires Service Géologique. Maroc 393, 106, 2000.

Hastie, A.R., Kerr, A.C., Pearce, J.A., Mitchell, S.F.: Classification of altered volcanic island arc rocks using immobile trace elements: development of the Th–Co discrimination diagram. Journal of Petrology. 48 (12), 2341–2357, https://doi.org/10.1093/ petrology/egm062, 2007.

Hefferan, K., Soulaimani, A., Samson, S. D., Admou, H., Inglis, J., Saquaque, A., … Heywood, N.: A reconsideration of Pan African orogenic cycle in the Anti-Atlas Mountains, Morocco. Journal of African Earth Sciences, 98, 34–46, https:// doi:10.1016/j.jafrearsci.2014.03.007, 2014.

Hefferan, K., Samson, S., Hietpas, J., Admou, H., Inglis, J., Saquaque, A., & Heywood, N.: A ~ 604 Ma depositional age for the Tiddiline conglomerate, Bou Azzer inlier, Morocco based on U–Pb dating of detrital zircon. Geol. Soc. Am, 44, 285, 2012.

Hodel, F., Triantafyllou, A., Berger, J., Macouin, M., Baele, J.M., Mattielli, N., Monnier, C., Trindade, R.I.F., Ducea, M.N., Chatir, A., Ennih, N., Langlade, J., Poujol, M.: The Moroccan Anti-Atlas ophiolites: Timing and melting processes in an intra-oceanic arc-back-arc environment. Gondwana Research. 86, 182–202, https://doi.org/10.1016/j.gr.2020.05.014, 2020.

Hofmann, A. W., Jochum, K. P., Seufert, M., and White, W. M.: Nb and Pb in oceanic basalts: new constraints on mantle evolution. Earth and Planetary science letters, 79(1-2), 33-45, https://doi.org/10.1016/0012-821X(86)90038-5, 1986.

Hooper, P.R., Bailey, D.G., McCarley Holder, G.A.: Tertiary calc-alkaline magmatism associated with lithospheric extension in the Pacific Northwest. J. Geophysical Research. 100 (B6), https://doi.org/10.1029/94JB03328, 10,303–10,319, 1995.

Horstwood, M. S., Košler, J., Gehrels, G., Jackson, S. E., McLean, N. M., Paton, C., ... and Schoene, B.: Community-derived standards for LA-ICP-MS U-(Th-) Pb geochronology–Uncertainty propagation, age interpretation and data reporting. Geostandards and Geoanalytical Research, 40(3), 311-332, https://doi.org/10.1111/j.1751-908X.2016.00379.x, 2016.

https://doi.org/10.5194/egusphere-2025-6178
Preprint. Discussion started: 18 December 2025

Ikenne, M., Söderlund, U., Ernst, R. E., Pin, C., Youbi, N., El Aouli, E. H., and Hafid, A.: A c. 1710 Ma mafic sill emplaced into a quartzite and calcareous series from Ighrem, Anti-Atlas – Morocco: Evidence that the Taghdout passive margin sedimentary group is nearly 1 Ga older than previously thought. Journal of African Earth Sciences. 127, 62–76, https://doi:10.1016/j.jafrearsci.2016.08.020, 2017.

Inglis, J.D., D'Lemos, R.S., Samson, S.D., Admou, H.: Geochronological constraints on Late Precambrian intrusion, metamorphism, and tectonism in the anti-atlas mountains. Journal of Geology. 113, 439–450, https://doi.org/10.1086/430242, 2005.

Karaoui, B., Breitkreuz, C., Mahmoudi, A., Youbi, N., Hofmann, M., Gärtner, A., & Linnemann, U.: U–Pb zircon ages from volcanic and sedimentary rocks of the Ediacaran Bas Draâ inlier (Anti-Atlas Morocco): Chronostratigraphic and provenance implications. Precambrian Research. 263, 43–58, https://doi:10.1016/j.precamres.2015.03.003, 2015.

Karaoui, B., Breitkreuz, C., Mahmoudi, A., and Youbi, N.: Physical volcanology, geochemistry and basin evolution of the Ediacaran volcano-sedimentary succession in the Bas Draâ inlier (Ouarzazate Supergroup, Western Anti-Atlas, Morocco). Journal of African Earth Sciences. 99, 307-331, https://doi.org/10.1016/j.jafrearsci.2014.06.022, 2014.

Large, R.R., Gemmell, J.B., Paulick, H., Huston, D.L.: The alteration box plot: a simple approach to understanding the relationship between alteration mineralogy and lithogeochemistry associated with volcanic-hosted massive sulfide deposits. Economic Geology. 96 (5), 957–971, https://doi.org/10.2113/gsecongeo.96.5.957, 2001.

Laurent, O., Martin, H., Moyen J.F., Doucelance, R.: The diversity and evolution of late-Archean granites: Evidence for the onset of a "modern-style" plate tectonics between 3.0 and 2.5 Ga. Lithos, 205, (pp. 208-235), https://doi.org/10.1016/j, 2014.

Leblanc, M., & Lancelot, J. R.: Interprétation géodynamique du domaine pan-africain (Précambrien terminal) de l'Anti-Atlas (Maroc) à partir de données géologiques et géochronologiques. Canadian Journal of Earth Sciences, 17(1), 142–155, https://doi:10.1139/e80-012, 1980.

Letsch, D., Houicha, M. E., von Quadt, A., and Winkler, W.: missing link in the peri-Gondwanan terrane collage: the Precambrian basement of the Moroccan Meseta and its lower Paleozoic cover. Canadian Journal of earth sciences, 55(1), 33-51, https://doi.org/10.1139/cjes-2017-0086, 2018.

Liégeois, J.P., Abdelsalam, M.G., Ennih, N., Ouabadi, A.: Metacraton: nature, genesis and behavior. Gondwana Res. 23 (1), 220–237, https://doi.org/10.1016/j. gr.2012.02.016, 2013.

Liégeois, J.P., Fekkak, A., Bruguier, O., Errami, E., Ennih, N.: The Lower Ediacaran (630–610 Ma) Saghro group: an orogenic transgressive basin development during the early metacratonic evolution of the Anti-Atlas (Morocco). In: IGCP485 4th meeting, Algiers, p. 57, 2006.

Liégeois, J. P., Navez, J., Hertogen, J., and Black, R.: Contrasting origin of post-collisional high-K calc-alkaline and shoshonitic versus alkaline and peralkaline granitoids. The use of sliding normalization. Lithos, 45(1-4), 1-28, https://doi.org/10.1016/S0024-4937(98)00023-1, 1998.

https://doi.org/10.5194/egusphere-2025-6178
Preprint. Discussion started: 18 December 2025

Linnemann, U., Ovtcharova, M., Schaltegger, U., Gärtner, A., Hautmann, M., Geyer, G., and Smith, J.: New high-resolution age data from the Ediacaran–Cambrian boundary indicate rapid, ecologically driven onset of the Cambrian explosion. Terra Nova, 31(1), 49-58, https://doi.org/10.1111/ter.12368, 2019.

Linnemann, U., Gerdes, A., Hofmann, M., Marko, L.: The Cadomian Orogen: Neoproterozoic to Early Cambrian crustal growth and orogenic zoning along the periphery of the West African Craton-Constraints from U-Pb zircon ages and Hf isotopes (Schwarzburg Antiform, Germany). Precambrian Research. 244, 236–278, https://doi.org/10.1016/j.precamres.2013.08.007, 2014.

M'arquez, A., Oyarzun, R., Doblas, M., and Verma, S. P.: Alkalic (ocean-island basalt type) and calc-alkalic volcanism in the Mexican volcanic belt: a case for plume-related magmatism and propagating rifting at an active margin?. Geology, 27(1), 51-54, https://doi.org/10.1130/0091-7613(1999)027<0051:AOIBTA>2.3.CO;2, 1999.

T. Campbell McCuaig., Kerrich, R., and Xie, Q.: Phosphorus and high field strength element anomalies in Archean high-magnesian magmas as possible indicators of source mineralogy and depth. Earth and Planetary Science Letters, 124(1-4), 221-239, https://doi.org/10.1016/0012-821X(94)00088-3, 1994.

Michard, A., Soulaimani, A., Ouanaimi, H., Raddi, Y., Brahim, L.A., Rjimati, E.C., Saddiqi, O.: Saghro Group in the Ougnat Massif (Morocco), an evidence for a continuous Cadomian basin along the northern West African Craton. Comptes Rendus Géosciences. 349 (2), 81–90, https://doi.org/10.1016/j.crte.2017.01.001, 2017.

Michard, A., Saddiqi, O., Chalouan, A., and de Lamotte, D. F. (Eds.).: Continental evolution: The geology of Morocco: Structure, stratigraphy, and tectonics of the Africa-Atlantic-Mediterranean triple junction (Vol. 116). Berlin: Springer, 2008.

Morris, G.A., Larson, P.B., Hooper, P.R.: 'Subduction style' magmatism in a non-subduction setting: the Colville Igneous Complex, NE Washington State, USA. Journal of Petrology. 41, 43–67, https://doi.org/10.1093/petrology/41.1.43, 2000.

Mrini, Z.: Chronologie (Rb-Sr, U-Pb), traçage isotopique (Sr-Nd-Pb) des sources de roches magmatiques éburnéenne, panafricaine et hercynienne du Maroc. Un-published thesis. University of Marrakech, Morocco, 200 p, 1993.

O'Connor, E.A., Barnes, R.P., Beddoe-Stephens, B., Fletcher, T., Gillespie, M.R., Hawkins, M.P., Loughlin, S.C., Smith, M., Smith, R.A., Waters, C.N., Williams, M.: Geology of the Drâa, Kerdous, and Boumalne Districts, Anti-Atlas. Keyworth, Nottingham British Geological Survey, Morocco, p. 324, 2010.

O'Reilly, S. Y., and Griffin, W. L.: Mantle metasomatism. Metasomatism and the chemical transformation of rock, 471-533, 2013.

Ouabid, M., Garrido, C.J.: Widespread Cadomian–Pan-African Ediacaran magmatism across the Moroccan Meseta: implication for the geodynamic evolution of the NW Gondwana margin. Precambrian Research. 387, https://doi.org/10.1016/j.precamres.2023.106992, 2023.

Ouguir, H., Macaudière, J., Dagallier, G. : Le Protérozoïque supérieur d'Imiter, Saghro oriental, Maroc : un contexte géodynamique d'arrière-arc. Journal of African Earth Sciences. 22 (2), 173–189, https://doi.org/10.1016/0899-5362(96)00002-4, 1996.

https://doi.org/10.5194/egusphere-2025-6178
Preprint. Discussion started: 18 December 2025

Pearce, J. A.: Geochemical fingerprinting of oceanic basalts with applications to ophiolite classification and the search for Archean oceanic crust. Lithos, 100(1-4), 14-48, https://doi.org/10.1016/j.lithos.2007.06.016, 2008.

Pearce, J.: Sources and settings of granitic rocks. Episodes, 19, 120-125, 1996.

Pearce, J. A., Harris, N. B., and Tindle, A. G.: Trace element discrimination diagrams for the tectonic interpretation of granitic rocks. Journal of petrology, 25(4), 956-983, https://doi.org/10.1093/petrology/25.4.956, 1984.

Pearce, J. A.: Role of the sub-continental lithosphere in magma genesis at active continental margins. Hawkesworth, C.J. and Norry, M.J., eds. Continental basalts and mantle xenoliths, Nantwich, Cheshire: Shiva Publications, pp. 230-249, 1983.

Pearce, J. A., and Norry, M. J.: Petrogenetic implications of Ti, Zr, Y, and Nb variations in volcanic rocks. Contributions to mineralogy and petrology, 69(1), 33-47, https://doi.org/10.1007/BF00375192, 1979.

Pearce, J. A., and Gale, G. H.: Identification of ore-deposition environment from trace-element geochemistry of associated igneous host rocks. Geological Society, London, Special Publications, 7(1), 14-24, https://doi.org/10.1144/GSL.SP.1977.007.01.03, 1977.

Pelleter, E., Cheilletz, A., Gasquet, D., Mouttaqi, A., Annich, M., Camus, Q., Deloule, E., Ouazzani, L., Bounajma, H., Ouchtouban, L.: U/Pb ages of magmatism in the Zgounder Epithermal Ag–Hg Deposit, Sirwa Window, Anti-Atlas, Morocco. In: Mineral Deposits of North Africa. Springer, pp. 143–165, https://doi.org/10.1007/978-3-319-31733-5_5, 2016.

Pereira, M. F., El Houicha, M., Chichorro, M., Armstrong, R., Jouhari, A., El Attari, A., and Silva, J. B.: Evidence of a Paleoproterozoic basement in the Moroccan Variscan belt (Rehamna massif, western Meseta). Precambrian Research, 268, 61-73, https://doi.org/10.1016/j.precamres.2015.07.010, 2015.

Pereira, M.F., Linnemann, U., Hofmann, M., Chichorro, M., Solá, A.R., Medina, J., Silva, J.B.: The provenance of Late Ediacaran and Early Ordovician siliciclastic rocks in the Southwest Central Iberian Zone: constraints from detrital zircon data on northern Gondwana margin evolution during the late Neoproterozoic. Precambrian Research. 192, 166–189, https://doi.org/10.1016/j.precamres.2011.10.019, 2012a.

Rojo-Pérez, E., Arenas, R., Fuenlabrada, J. M., Novo-Fernández, I., Martínez, S. S., Moreno-Martín, D., and Fernández, R. D.: Lower Cambrian magmatism in the SW Iberian sector of the African–Gondwana margin: geochemical and isotopic keys to incipient tectonic switching, https://doi.org/10.1144/SP542-2022-294, 2024.

Saadi, A.: Contribution à l'étude écologique de deux hydrosystèmes temporaires saumâtres du Maroc : Zima et Sedd-El-Messjoun (Bassin de la Bahira). PhD thesis, Semlalia Faculty, University of Cady Ayyad, Marrakech, Morocco, 1985.

Saccani, E.: A new method of discriminating different types of post-Archean ophiolitic basalts and their tectonic significance using Th-Nb and Ce-Dy-Yb systematics. Geoscience Frontiers, 6(4), 481-501, https://doi.org/10.1016/j.gsf.2014.03.006, 2015.

Safonova, I., Maruyama, S., Kojima, S., Komiya, T., Krivonogov, S., and Koshida, K.: Recognizing OIB and MORB in accretionary complexes: A new approach based on ocean plate stratigraphy, petrology and geochemistry. Gondwana Research, 33, 92-114, https://doi.org/10.1016/j.gr.2015.06.013, 2016.

https://doi.org/10.5194/egusphere-2025-6178
Preprint. Discussion started: 18 December 2025

Samson, S. D., Inglis, J. D., D'Lemos, R. S., Admou, H., Blichert-Toft, J., and Hefferan, K.: Geochronological, geochemical, and Nd–Hf isotopic constraints on the origin of Neoproterozoic plagiogranites in the Tasriwine ophiolite, Anti-Atlas orogen, Morocco. Precambrian Research, 135(1-2), 133–147, https://doi:10.1016/j.precamres.2004.08.003, 2004.

Saunders, A. D., and Tarney, J.: Geochemical characteristics of basaltic volcanism within back-arc basins. Geological Society, London, Special Publications, 16(1), 59-76, https://doi.org/10.1144/GSL.SP.1984.016.01.05, 1984.

Schulte, B., Boger, S.D., Benziane, F., Yazidi, A., Fanning, C.M.: The Ouarzazate Supergroup and its plutonic keel: the relics of an Ediacaran silicic large igneous province in North Africa. Journal of the Geological Society. London. 179, 5, https://doi.org/10.1144/ jgs2021-114, 2022.

Shand, S. J.: Eruptive rocks; their genesis, composition, classification, and their relation to ore-deposits with a chapter on meteorite. New York: John Wiley & Sons, 1943.

Sharman, G. R., and Malkowski, M. A.: Modeling apparent Pb loss in zircon U–Pb geochronology. Geochronology, 6(1), 37-51, https://doi.org/10.5194/gchron-6-37-2024, 2024.

Shervais, J. W.: Ti-V plots and the petrogenesis of modern and ophiolitic lavas. Earth and planetary science letters, 59(1), 101-118, https://doi.org/10.1016/0012-821X(82)90120-0, 1982.

Shinjo, R., and Kato, Y.: Geochemical constraints on the origin of bimodal magmatism at the Okinawa Trough, an incipient back-arc basin. Lithos, 54(3-4), 117-137, https://doi.org/10.1016/S0024-4937(00)00034-7, 2000.

Soulaimani, A., Ouanaimi, H., Saddiqi, O., Baidder, L., and Michard, A.: The Anti-Atlas Pan-African Belt (Morocco): Overview and pending questions. Comptes Rendus Géoscience, https://doi:10.1016/j.crte.2018.07.002, 2018.

Stern, R. J.: A reinterpretation of the past 2.5 billion years of Earth's tectonic history: Two episodes each of plate and single-lid tectonics. Geological Society of America Bulletin, https://doi.org/10.1130/B37966.1, 2024.

Sun, S. S., and McDonough, W. F.: Chemical and isotopic systematics of oceanic basalts: implications for mantle composition and processes. Geological Society, London, Special Publications, 42(1), (pp. 313-345), https://doi.org/10.1144/GSL.SP.1989.042.01.19, 1989.

Tahiri, A., Montero, P., El Hadi, H., Poyatos, D. M., Azor, A., Bea, F., and Lodeiro, F. G.: Geochronological data on the Rabat–Tiflet granitoids: their bearing on the tectonics of the Moroccan Variscides. Journal of African Earth Sciences, 57(1-2), 1-13, https://doi.org/10.1016/j.jafrearsci.2009.07.005, 2010.

Taylor, S. R., and McLennan, S. M.: The geochemical evolution of the continental crust. Reviews of geophysics, 33(2), 241-265, https://doi.org/10.1029/95RG00262, 1995.

Thomas, R. J., Fekkak, A., Ennih, N., Errami, E., Loughlin, S. C., Gresse, P. G., Liégeois, J.-P.: A new lithostratigraphic framework for the Anti-Atlas Orogen, Morocco. Journal of African Earth Sciences, 39(3-5), 217–226, https://doi:10.1016/j.jafrearsci.2004.07.046, 2004.

Thomas, R. ., Chevallier, L. ., Gresse, P. ., Harmer, R. ., Eglington, B. ., Armstrong, R. ., Ingram, B.: Precambrian evolution of the Sirwa Window, Anti-Atlas Orogen, Morocco. Precambrian Research, 118(1-2), 1–57, https://doi:10.1016/s0301-9268(02)00075-x, 2002.

https://doi.org/10.5194/egusphere-2025-6178
Preprint. Discussion started: 18 December 2025

Thomas, R.J., De Beer, C.H., Chevallier, L.P., De Kock, G.S., Gresse, P.G.: Notice Explicative de la Carte Géologique du Maroc au 1/50 000 feuille Assarag. Notes et Mémoires Service Géologique. Maroc 392, 84, 2000a.

Touil, A., Hafid, A., Moutte, J., and El Boukhari, A.: Petrology and geochemistry of the Neoproterozoic Siroua granitoids (central Anti-Atlas, Morocco): evolution from subduction-related to within-plate magmatism. Geological Society, London, Special Publications, https://doi.org/10.1144/SP297.13, 2008.

Touil, A., El-Boukhari, A., Bilal, E., and Moutte, J. : Les tholeiites a affinité alcaline du secteur ouest du Siroua (Anti-Atlas central, Maroc): témoins d'une distension au Néoprotérozoïque. Journal of African Earth Sciences, 29(4), 699-713, https://doi.org/10.1016/S0899-5362(99)00125-6, 1999.

Toummite, A., Liégeois, J.P., Gasquet, D., Bruguier, O., Beraaouz, E.H., Ikenne, M.: Field, geochemistry and Sr-Nd isotopes of the Pan-African granitoids from the Tifnoute Valley (Sirwa, Anti-Atlas, Morocco): a post-collisional event in a metacratonic setting. Mineralogy and Petrology. 107 (5), 739–763, https://doi.org/10.1007/ s00710-012-0245-3, 2013.

Triantafyllou, A., Berger, J., Baele, J.-M., Diot, H., Ennih, N., Plissart, G., Vandycke, S.: The Tachakoucht–Iriri–Tourtit arc complex (Moroccan Anti-Atlas): Neoproterozoic records of polyphased subduction-accretion dynamics during the Pan-African orogeny. Journal of Geodynamics, 96, 81–103, https://doi.org/10.1016/j.jog.2015.07.004, 2016.

Tuduri, J., Chauvet, A., Barbanson, L., Bourdier, J.L., Labriki, M., Ennaciri, A., Badra, L., Dubois, M., Ennaciri-Leloix, Ch., Sizaret, S., Maacha, L.: The Jbel Saghro au (–Ag, Cu) and Ag–Hg Metallogenetic Province: product of a Long-Lived Ediacaran Tectono-Magmatic Evolution in the Moroccan Anti-Atlas. Minerals, 8 (12), 592, https://doi.org/10.3390/min8120592, 2018.

Vasey, D. A., Cowgill, E., & Cooper, K. M.: A preliminary framework for magmatism in modern continental back-arc basins and its application to the Triassic-Jurassic tectonic evolution of the Caucasus. Geochemistry, Geophysics, Geosystems, 22(6), e2020GC009490, https://doi.org/10.1029/2020GC009490, 2021.

Vermeesch, P.: IsoplotR: A Free and Open Toolbox for Geochronology. Geoscience Frontiers. 9 (5), 1479–1493, https://doi.org/10.1016/j.gsf.2018.04.001, 2018.

Walsh, G.J., Aleinikoff, J.N., Harrison, R.W., Yazidi, A., Burton, W.C., Quick, J.E., Benziane, F., Yazidi, A., Saadane, A.: Neoproterozoic tectonic evolution of the Jebel Saghro and Bou Azzer—El Graara inliers, eastern and central Anti-Atlas, Morocco. Precambrian Research. 216, 23–62, https://doi.org/10.1016/j. precamres.2012.06.010, 2012.

Walsh, G. J., Aleinikoff, J. N., Benziane, F., Yazidi, A., & Armstrong, T. R.: U–Pb zircon geochronology of the Paleoproterozoic Tagragra de Tata inlier and its Neoproterozoic cover, western Anti-Atlas, Morocco. Precambrian Research, 117(1-2), 1-20, https://doi.org/10.1016/S0301-9268(02)00044-X, 2002.

Wilson, M. (Ed.).: Igneous petrogenesis. Dordrecht: Springer Netherlands, 1989.

Winchester, J. A., and Floyd, P. A.: Geochemical discrimination of different magma series and their differentiation products using immobile elements. Chemical geology, 20, (pp. 325-343), https://doi.org/10.1016/0009-2541(77)90057-2, 1977.

Wood, D. A.: The application of a Th-Hf-Ta diagram to problems of tectonomagmatic classification and to establishing the nature of crustal contamination of basaltic lavas of the British Tertiary Volcanic Province. Earth and planetary science letters, 50(1), 11-30, https://doi.org/10.1016/0012-821X(80)90116-8, 1980.

https://doi.org/10.5194/egusphere-2025-6178
Preprint. Discussion started: 18 December 2025

Yajioui, Z., Karaoui, B., Chew, D., Breitkreuz, C., Mahmoudi, A.: U–Pb zircon geochronology of the Ediacaran volcano-sedimentary succession of the NE Saghro inlier (Anti-Atlas, Morocco): chronostratigraphic correlation on the northwestern margin of Gondwana. Gondwana Research. 87, 263–277, https://doi.org/10.1016/j. gr.2020.06.015, 2020.

Youbi, N., Ernst, R.E., Soderlund, U., Boumehdi, M.A., Ait Lahna, A., Tassinari, C.C.G., El Moume, W., Bensalah, M.K.: The Central Iapetus magmatic province: an updated review and link with the ca. 580 Ma Gaskiers glaciation. In: Adatte, T., Bond, D.P.G., Keller, G. (Eds.), Mass Extinctions, Volcanism, and Impacts: New Developments: Geological Society of America Special Paper, 544, pp. 35–66, https://doi.org/10.1130/2020.2544(02), 2020.